

## RESEARCH ARTICLE

## Decreasing mitochondrial RNA polymerase activity reverses biased inheritance of hypersuppressive mtDNA

Daniel Corbi<sup>1\*</sup>, Angelika Amon<sup>1,2†</sup>

**1** David H. Koch Institute for Integrative Cancer Research and the Department of Biology, Massachusetts Institute of Technology, Cambridge, Massachusetts, United States of America, **2** Howard Hughes Medical Institute, Massachusetts Institute of Technology, Cambridge, Massachusetts, United States of America

† Deceased.

\* [dan.corbi@gmail.com](mailto:dan.corbi@gmail.com)

## OPEN ACCESS

**Citation:** Corbi D, Amon A (2021) Decreasing mitochondrial RNA polymerase activity reverses biased inheritance of hypersuppressive mtDNA. *PLoS Genet* 17(10): e1009808. <https://doi.org/10.1371/journal.pgen.1009808>

**Editor:** David M. MacAlpine, Duke University Medical Center, UNITED STATES

**Received:** April 26, 2021

**Accepted:** September 7, 2021

**Published:** October 19, 2021

**Peer Review History:** PLOS recognizes the benefits of transparency in the peer review process; therefore, we enable the publication of all of the content of peer review and author responses alongside final, published articles. The editorial history of this article is available here: <https://doi.org/10.1371/journal.pgen.1009808>

**Copyright:** © 2021 Corbi, Amon. This is an open access article distributed under the terms of the [Creative Commons Attribution License](https://creativecommons.org/licenses/by/4.0/), which permits unrestricted use, distribution, and reproduction in any medium, provided the original author and source are credited.

**Data Availability Statement:** Most relevant data is contained within the manuscript; for a few datasets of raw RNA or DNA sequencing please see the following links: SMRT sequencing of Hypersuppressive mtDNAs: <https://doi.org/10.1371/journal.pgen.1009808>

## Abstract

Faithful inheritance of mitochondrial DNA (mtDNA) is crucial for cellular respiration/oxidative phosphorylation and mitochondrial membrane potential. However, how mtDNA is transmitted to progeny is not fully understood. We utilized hypersuppressive mtDNA, a class of respiratory deficient *Saccharomyces cerevisiae* mtDNA that is preferentially inherited over wild-type mtDNA (*rho+*), to uncover the factors governing mtDNA inheritance. We found that some regions of *rho+* mtDNA persisted while others were lost after a specific hypersuppressive takeover indicating that hypersuppressive preferential inheritance may partially be due to active destruction of *rho+* mtDNA. From a multicopy suppression screen, we found that overexpression of putative mitochondrial RNA exonuclease *PET127* reduced biased inheritance of a subset of hypersuppressive genomes. This suppression required *PET127* binding to the mitochondrial RNA polymerase *RPO41* but not *PET127* exonuclease activity. A temperature-sensitive allele of *RPO41* improved *rho+* mtDNA inheritance over a specific hypersuppressive mtDNA at semi-permissive temperatures revealing a previously unknown role for *rho+* transcription in promoting hypersuppressive mtDNA inheritance.

## Author summary

Functional mitochondrial DNA is important for cells to maintain fitness and too much damaged mitochondrial DNA can cause debilitating diseases in humans. Inheritance of mitochondrial DNA from cell to cell as they divide is still a poorly understood process especially when multiple mitochondrial DNA forms are present. Here, we study a defective yeast mitochondrial DNA with the unusual property that it is inherited almost exclusively when present with functional mitochondrial DNA inside the same cell. We noticed that the functional mitochondrial DNA becomes damaged which suggests the defective mitochondrial DNA somehow promotes the destruction of the functional mitochondrial DNA when both are present; whereas, the current thinking is that the defective mitochondrial DNA is simply made faster than functional mitochondrial DNA. Also, we found that

5061/dryad.547d7wm8v RNA sequencing characterizing nuclease dead Pet127 mutants: <https://doi.org/10.5061/dryad.cfxpvnv5z> RNA sequencing of overexpressed pet127 mutants: <https://doi.org/10.5061/dryad.mw6m905xg>.

**Funding:** AA received an award from the National Institute of General Medical Sciences (GM118066) which helped fund this project. <https://www.nigms.nih.gov/> AA was an investigator of the Howard Hughes Medical Institute which helped fund this project. <https://www.hhmi.org/> The funders had no role in study design, data collection and analysis, decision to publish, or preparation of the manuscript.

**Competing interests:** The authors have declared that no competing interests exist. Author Angelika Amon was unable to confirm their authorship contributions. On their behalf, the corresponding author has reported their contributions to the best of their knowledge.

a reduction of functional mitochondrial DNA gene expression protects the functional mitochondrial DNA from destruction by defective mitochondrial DNA revealing a novel role for functional mitochondrial DNA in the preferential inheritance of defective mitochondrial DNA. Both findings suggest there is an interplay between the genomes, either by competition for resources or interaction between the genomes, which has not been previously considered.

## Introduction

The mitochondrion is an essential eukaryotic organelle and the site for many critical metabolic reactions such as iron-sulfur cluster metabolism, heme biosynthesis, the TCA cycle, and cellular respiration/oxidative phosphorylation [1–3]. Most mitochondrial proteins are encoded by the nuclear DNA, made in the cytosol and imported into mitochondria [4,5]. However, mitochondria also have their own genome (mtDNA) containing a small number of genes that encode core components of complexes involved in cellular respiration/oxidative phosphorylation and machinery to translate those genes [6,7]. Unlike nuclear DNA, there are many copies of mtDNA per cell and, in *Saccharomyces cerevisiae*, both linear and circular forms of mtDNA are present [8–10].

In budding yeast, respiration-capable mtDNA (*rho*<sup>+</sup>) encodes genes critical for activity of the mitochondrial ribosome (*VARI*, *15srRNA*, *21srRNA*, *tRNA*), components of mitochondrial electron transport chain (ETC) complexes: complex III (*COB*), complex IV (*COX1*, *COX2*, *COX3*), and components of the ATP synthase complex (*ATP6*, *ATP8*, *ATP9*) [6,7]. Loss of respiratory function caused either by partial disruption of mtDNA (*rho*<sup>-</sup>) or total loss of the mtDNA (*rho*<sup>0</sup>) results in impaired cellular respiration/oxidative phosphorylation and a slower colony growth phenotype. This reduced growth occurs even in non-respiratory conditions and is called petiteness [11,12]. Although mtDNA must be faithfully replicated, maintained, and segregated to progeny to maintain cellular fitness, mtDNA inheritance is not fully understood [13–17].

An approach to understand mtDNA inheritance comes from studies of mutant mtDNA in yeast that exhibit extremely biased inheritance. When two yeast cells mate, their cytoplasm fuse and each haploid parent contributes mitochondria with mtDNA to the resulting diploid daughter cell [10]. In most cases, mating between yeast parents containing *rho*<sup>+</sup> respiration competent mtDNA and parents containing respiration incompetent *rho*<sup>-</sup> or *rho*<sup>0</sup> mtDNA results in almost entirely respiration competent progeny, indicating strong inheritance of *rho*<sup>+</sup> mtDNA [18]. Some *rho*<sup>-</sup> genomes may persist in the progeny after mating *rho*<sup>+</sup> and *rho*<sup>-</sup> yeast, and these *rho*<sup>-</sup> genomes are called partial suppressives [18,19]. However, a subset of *rho*<sup>-</sup> mutants, called hypersuppressive (HS) mtDNA, are extremely biased in their inheritance. When mated with *rho*<sup>+</sup> cells, cells with HS mtDNA result in greater than 95% *rho*<sup>-</sup> progeny [18,20]. HS mtDNA mutants display preferential mtDNA inheritance despite giving rise to slow-growing respiration-incompetent cells. Thus, understanding how HS mutants hijack mtDNA inheritance machinery provides insights into how mtDNA inheritance works.

Characterization of HS *rho*<sup>-</sup> mutant genomes showed that they consist entirely of short (less than 2.5kbp) tandem repeats of one of three regions of high sequence similarity from the *rho*<sup>+</sup> genome [21–23]. As the HS genomes found in the diploid progeny after mating *rho*<sup>+</sup> and HS *rho*<sup>-</sup> are unchanged from those in the HS *rho*<sup>-</sup> parent, a prevailing theory is that HS mutants confer a replication advantage over *rho*<sup>+</sup> [19,22,24]. The regions of the *rho*<sup>+</sup> genome present in HS mutants are thought to be origins of replication, having similarities to mammalian

mtDNA replication origins [25–27], and are known as *ORI* or rep regions [23,28–30] despite not being necessary for mtDNA stability [31]. According to the replication advantage theory, *HS* mtDNAs have a higher density of *ORI* regions, because of the small tandem repeats, conferring a replicative advantage over *rho+* mtDNA upon mating. Preferential inheritance of damaged mtDNA has been implicated in the progression of human mtDNA diseases and aging [32,33]. As there is similarity between *HS* origins in yeast and the heavy strand origin in mammals [26], there is reason to believe that preferential inheritance of mtDNA is similar. So, by understanding the principles of biased mtDNA inheritance in yeast we may gain insights into disease contexts.

One model supporting the replication advantage theory is the RNA priming hypothesis for mtDNA replication. The *rho+* genomic regions corresponding to the *HS ORI*s direct transcription of a ~300bp non-coding RNA that is cleaved and can be used as a primer for *in vitro* DNA replication [7,29,30]. The *rho+* genome has eight regions of *ORI* homology [34,35], but only the three or four *HS ORI*s (2, 3, 5 and, in some strain backgrounds, 1) are known to make such an RNA [7,27]. The presence of only RNA producing *ORI*s in *HS* mutants suggests that *HS* genomes are replicated by RNA priming initiation and this mechanism confers their replication advantage over *rho+* genomes [7].

There is, however, evidence against the RNA priming hypothesis for mtDNA replication. Certain *rho-* mtDNA genomes are stably replicated despite lacking either an *ORI* promoter or the mitochondrial RNA polymerase [31,36,37]. Also, *HS* mtDNA was shown to still be preferentially inherited without the mitochondrial RNA polymerase [38]; although, there are serious caveats to this experiment. Thus, both replication and *HS* biased inheritance need not work through *ORI* RNA or, more broadly, an RNA intermediate. A recombination-based replication model has been proposed to resolve this discrepancy [39,40].

There are some indications that the replication advantage model cannot entirely explain *HS* biased inheritance. The replication rate of a panel of partially suppressive *rho-* mutants fails to correlate with the extent of inheritance bias [41]. Also, increasing the pool of available nucleotides reduces the *HS* inheritance bias [42]. This suggests that alternative models of biased inheritance are partially or wholly responsible for the *HS* phenotype.

Here, we uncover that a specific *HS* mtDNA causes DNA damage to *rho+* mtDNA. Also, we perform a forward genetic suppressor screen using a high-copy genomic library to look for multicopy suppressors of *HS*. We find that overexpression of mitochondrial RNA exonuclease *PET127* suppresses the *HS* inheritance bias of certain *HS* alleles by negatively regulating mitochondrial RNA polymerase *RPO41*.

## Results

### Characterization of *HS* mtDNA

To generate *HS* mutants, we first used low-level ethidium bromide (EtBr) treatment for short periods of time to generate petite colonies (S1A Fig, [11]). Next, to identify which petite colonies were *HS rho-*, we mated the newly generated petite strains to *rho+* cells and monitored the color of the diploid strains. Monitoring color allowed us to take advantage of the fact that respiration is required for biosynthesis of a red purine analog that turns *ade2-1* yeast red [43]. Thus, while *rho+ ade2-1* yeast colonies turn red, *rho0* or *rho- ade2-1* colonies remain white [43]. By definition, *HS* cells will result predominantly in *rho-* diploids upon mating with *rho+*. Thus, we identified *HS* alleles by looking for white colonies upon mating petite colonies with *rho+* (S1B Fig). We validated the potential *HS* alleles using a quantitative mating assay where we mated the cells, plated the cells to select for diploids, and replica-plated the diploids to medium requiring respiration. We then can assess the fraction of mated cells which retain

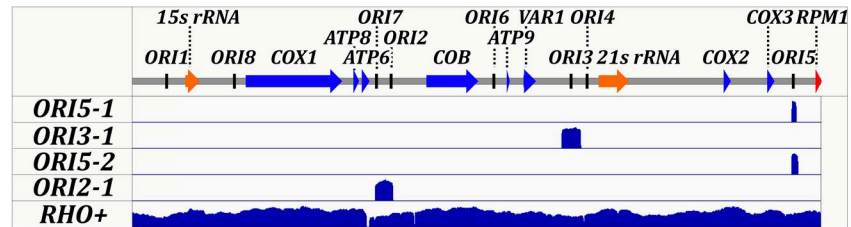


**Fig 1. Generation and Characterization of HS Alleles.** Mitochondria DNA from HS1b (*ORI5-1*), HS3b (*ORI5-2*), HS6a (*ORI3-1*), HS11b (*ORI2-1*), and *rho+* control cells was sequenced using pacific biosciences sequencing technology and mapped back to reference genome. Reads from *HS ORI5-1* mapped to base pairs 82,101 to 82,615 of the wild type reference genome. *HS ORI3-1* mapped to 53,495 to 55,836. *HS ORI5-2* mapped to 82,095 to 82,817. *HS ORI2-1* mapped to 30,305 to 32,497. Scale bar ranges are 0 to 1619 for *HS ORI5-1*, 0 to 1474 for *HS ORI5-1*, 0 to 1111 for *HS ORI3-1*, 0 to 660 for *HS ORI2-1* and 0 to 305 for *rho+*.

<https://doi.org/10.1371/journal.pgen.1009808.g001>

*rho+* mtDNA by dividing the number of cells which grow on respiration requiring medium by the total number of cells on the diploid selection (S1C Fig, [18]).

Four of the HS clones were further characterized. We performed sequencing using single molecule real-time (SMRT) sequencing of the mtDNA from each clone and the *rho+* parent and mapped the sequenced DNA back to the wild-type reference genome (Fig 1). In accordance with past literature, we found the four clones mapped to the mtDNA at *ORI* containing regions. We renamed the alleles *HS ORI5-1*, *HS ORI5-2* (spanning all of *HS ORI5-1*), *HS ORI3-1*, and *HS ORI2-1*. The long reads facilitated by SMRT sequencing allowed us to confirm that each of the HS alleles are tandem *ORI* repeats completely lacking other regions of the *rho+* genome.

### The presence of *HS ORI5-1* mtDNA damages *rho+* mtDNA

Previous studies showed that *HS* mtDNA eliminates *rho+* mtDNA, however it is unclear how the *rho+* mtDNA is eliminated [19,22]. To shed light on the fate of *rho+* mtDNA, we asked what happens to different regions of *rho+* mtDNA shortly after introducing *HS* mtDNA to cells. We mated *HS ORI5-1* and *rho+* parents and used PCR to ask if regions of *rho+* mtDNA are still present in the daughter colony. We found three types of respiration incompetent colonies. Five colonies had no observable *rho+* regions (Fig 2: Colonies 2, 3, 4, 9, 12), which is expected for the final state of cells after complete takeover of *HS* mtDNA [19,22]. Four colonies maintained *rho+* mtDNA from all regions assayed (Fig 2: Colonies 6, 7, 8, and 10) much like those from the *rho0* mated control and the *rho+* parent. This was unexpected as respiration incompetent colonies from a *rho+* and *HS* cross were thought to entirely contain *HS* genomic DNA [24]. Lastly, we observed three colonies that lost some but not all regions of the *rho+* genome (Fig 2: Colony 1 losing Cox1-Cterm; Colony 5 losing Cox2, Cox3, and Cox1-Cterm; and Colony 11 losing Cox2, Cox3, Atp9, and Cox1-Cterm). All colonies were assayed for a control nuclear genomic region. Only *rho0* parental controls failed to contain any mitochondrial DNA assayed by a nonspecific *ORI* primer set that detects the *ORI5* locus present in both *rho+* and *HS ORI5-1* mtDNA (Fig 2). The sensitivity of the *rho+* detecting primers was assayed by five-fold serial dilutions of *rho+* parental DNA into *HS ORI5-1* parental DNA (S2 Fig). The most sensitive primers are Cox1-Nterm, Cox3 and Atp9 which were all able to detect 0.64ng of *rho+* template. Whereas, Cox1-Cterm and Cox2 failed to detect 3.2 ng of parental DNA. For colony 1, a Cox2 band is present but not a Cox1-Cterminal band and as Cox2 is less sensitive than Cox1 C-terminal that indicates a loss of the Cox1 C-terminal region. For colony 5 and colony 11, Cox3, the most sensitive primer, is missing despite the presence of the Cox1-Nterm bands indicating a loss of Cox3. From these data we conclude that *rho+* mtDNA is lost in a

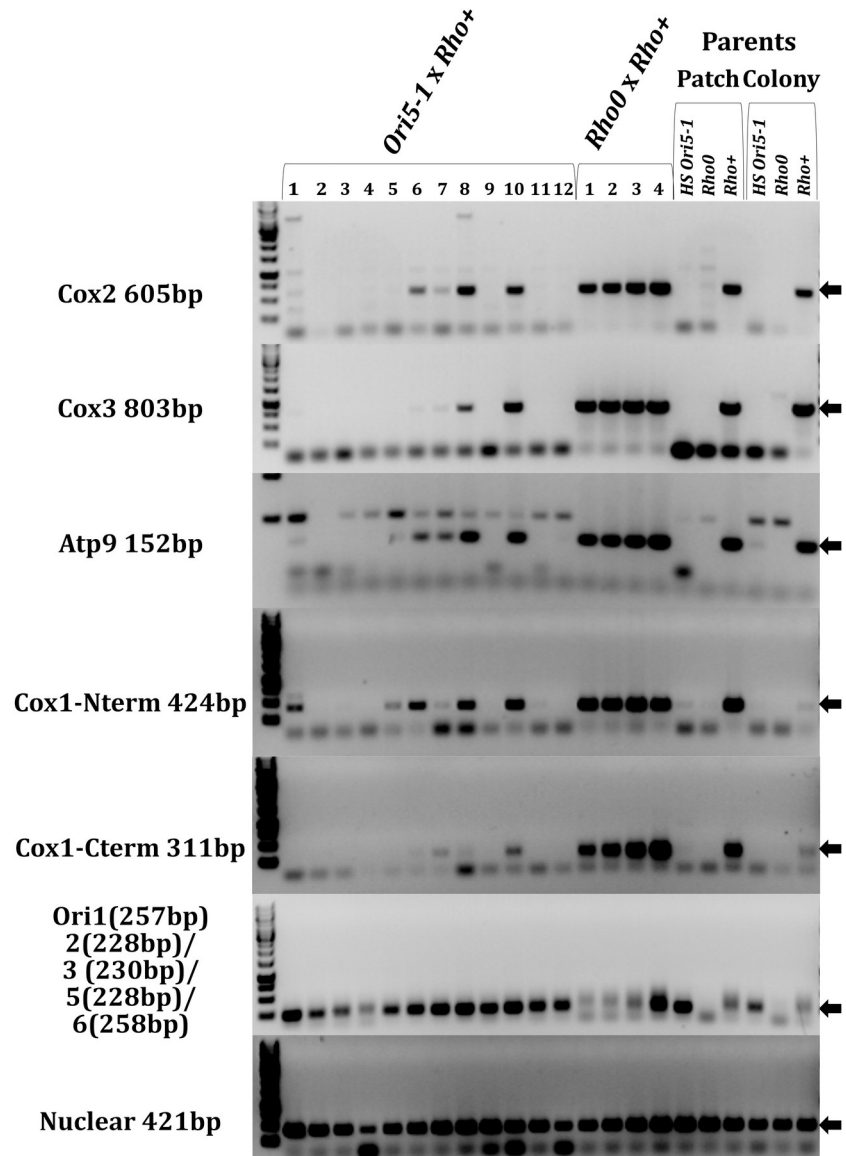


**Fig 2. Colony PCR after *HS* x *rho+* Reveals Remnants of *rho+* mtDNA.** The indicated strains were mated and plated on diploid selection medium. The parent strains were plated to single colonies. After two days, individual colonies were scraped off the plates, and DNA was isolated. Genomic DNA was normalized, and PCRs were performed with primer sets amplifying the indicated loci. Reactions were run on agarose gels and stained with ethidium bromide. Arrows indicate the size of the intended product.

<https://doi.org/10.1371/journal.pgen.1009808.g002>

piecemeal fashion rather than all at once. This fragmented loss of mtDNA cannot be explained by a replicative advantage, therefore *HS* mtDNA somehow causes genomic damage to the intact mtDNA.

### ***PET127* overexpression suppresses the biased inheritance of a subset of *HS* genomes**

To better understand the factors governing mtDNA inheritance, we performed a whole-genome screen to identify suppressors of the biased inheritance of *HS* mutants. We utilized the *HS ORI5-1* allele for our suppression screen as many prior studies of *HS* mtDNA have

focused on *ORI5* alleles [39,40,42,44]. Specifically, wild-type *rho+* cells were transformed with a high-copy plasmid library [45], mated with the *HS ORI5-1* strain, and assayed using the same red/white colony phenotype that we used to isolate HS alleles (Fig 3A) [43]. Most diploid colonies were white due to the dominant inheritance of the *HS ORI5-1* mutant. However, four plasmids were identified that repeatedly led to the formation of red *rho+* colonies, indicating suppression of the *HS* biased inheritance. Two colonies contained plasmids bearing a region of chromosome XV with four shared genes: the 3' region of *RTS1*, putative gene *YOR015W*, *ERP4*, and *PET127* (one plasmid fully encompassing *PET127*, one containing the 5' 2254 bp out of the 2403 bp coding sequence of *PET127*) (S3A Fig).

We mapped the gene required for suppression on the plasmids. The region of *RTS1* in the plasmids does not contain a functional promoter, and *YOR015W* is only a putative gene with a start site 45 bp from the end of *RTS1*, making them less likely candidates. Thus, we focused on *ERP4* and *PET127* and quantitatively assessed their individual suppressive capabilities (Fig 3B). An empty vector in the *rho+* background showed  $1.7\% \pm 1.3$  *rho+* colonies when mated to *HS ORI5-1* but yeast containing the parent plasmid isolated from the screen recovered  $42\% \pm 2.1$  *rho+* colonies. A plasmid containing either *ERP4* or *PET127* showed  $3.5\% \pm 3.2$  and  $43\% \pm 5.4$  *rho+* colonies respectively, implicating *PET127* as the sole causative suppressive gene. The *rho+* colonies resulting from high-copy *PET127* suppression grew in a subset region of the original diploid parental colony (S3B Fig). This *rho+* subset was not sectored in any discernable pattern, and, as the high-copy plasmid is selected for on the diploid selection plates and should not be lost in large sections of the colony, indicates that there is stochasticity in how high-copy *PET127* prevents HS takeover. Mating *rho+* yeast containing the suppressive plasmid or a plasmid containing *PET127* to the *rho0* control did not result in a reduction of *rho+* colonies. This indicated that the high-copy *PET127* plasmid expression level from its endogenous promoter did not result in the loss of mtDNA in the *rho+* haploid parent despite prior literature showing expression of *PET127* from the strong *ADC1* promoter on multicopy plasmids can result in petite cells [46]. From these data, we conclude that overexpression of *PET127* is a suppressor of the preferential inheritance of *HS ORI5-1*.

Next, we asked if overexpression of *PET127* could suppress the phenotype of the other *HS rho-* mitochondrial genomes using the same approach. We mated *rho+* strains containing *PET127* with the one clone from each strain in the panel of HS alleles in S1C Fig and determined the number of *rho+* diploid colonies (Fig 3C). The suppressive effect of *PET127* overexpression was strongest for *HS ORI5-1* but also significant in *HS2b*, *HS5b*, *HS8b*, and *HS10b*. The effect on all other HS alleles was insignificant including *HS ORI5-2* which contains the whole region of *HS ORI5-1*. We genotyped HS alleles using a PCR strategy with primers which have homology to *ORI2*, *ORI3*, and *ORI5* but have 3' ends facing each other rather than 5' ends [47]. As HS alleles are repetitive in nature, this strategy should generate a product spanning the length of a repeat except for the nucleotides between the 3' primer ends. This strategy did not produce products for all HS alleles, but determined that the *PET127* sensitive strain *HS10b* contains *ORI2* DNA indicating that *PET127* sensitivity is not due to the features of one particular ORI.

We wondered whether either the specific HS allele or a background nuclear mutation is responsible for determining which strains are sensitive to high-copy *PET127* suppression. To determine which hypothesis is correct, we shuttled the mtDNA of *HS ORI5-1* and *HS ORI5-2* alleles to the same independently generated *rho0* recipient by cytoduction (mating with yeast defective in nuclear fusion to allow for transfer of cytoplasmic factors without changing nuclear genotype) and tested the suppression by quantitatively mating the resulting strains to *rho+* cells overexpressing *PET127* [48]. This experiment resulted in similar levels of *rho+* colonies post-mating (S3C Fig), indicating that differences in the extent of high-copy *PET127*

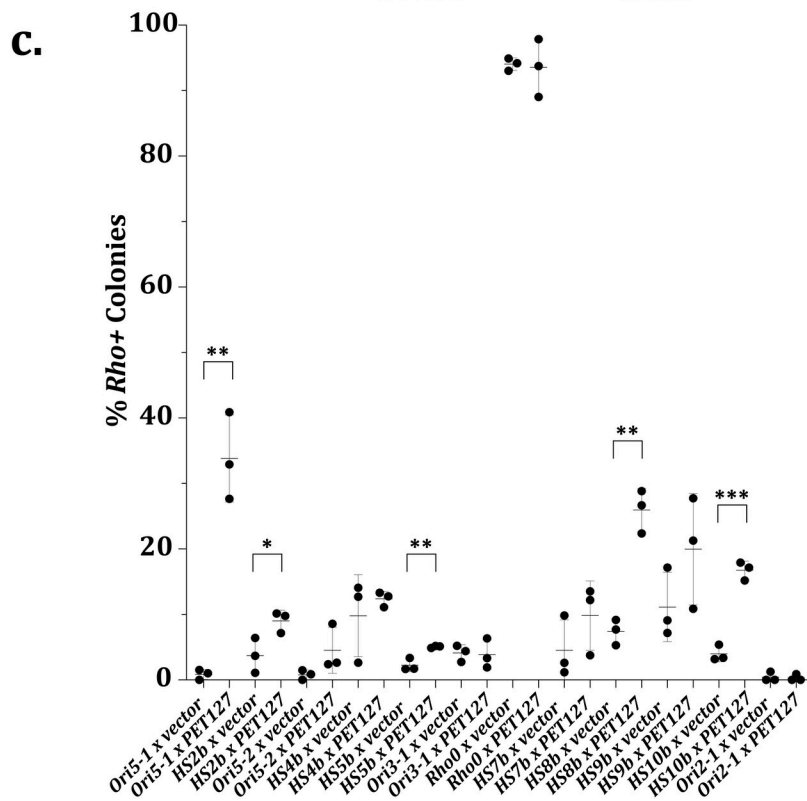
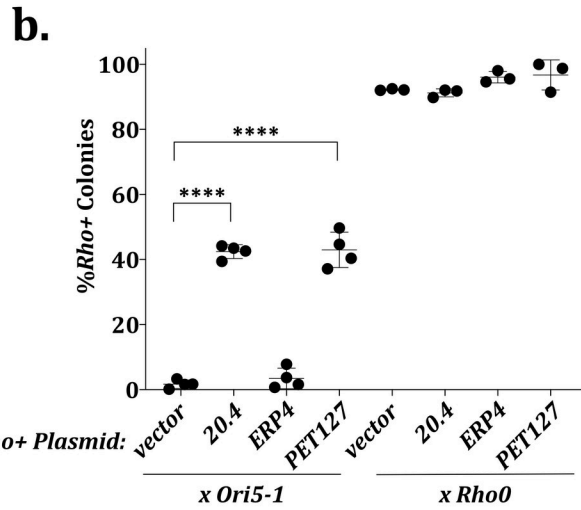
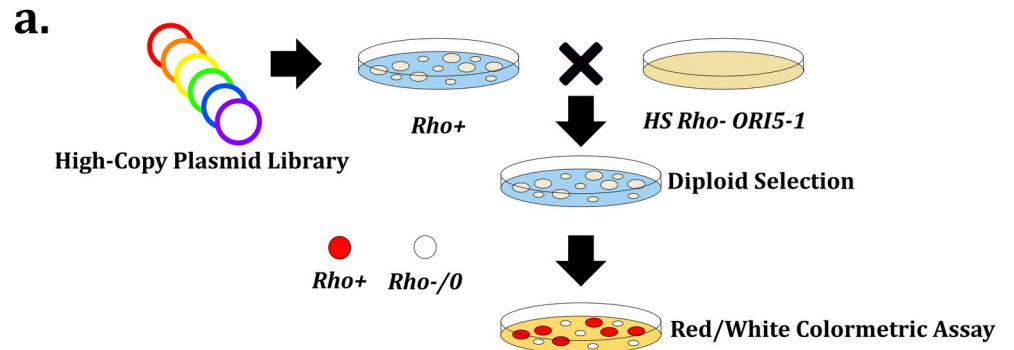


**Fig 3. High-copy *PET127* is a Suppressor of *HS rho*- Preferential Inheritance.** A. *Rho*<sup>+</sup> cells were transformed with Yep13 high-copy library [45] and 10,967 colonies were plated. Plasmid containing colonies were mated with lawns of *HS Ori5-1*, replica plated to diploid selection medium and replica plated again to YEPD with no additional adenine. We identified 154 red colonies initially, however only 5 colonies were red after repetition of the assay. Four of the five colonies showed suppression and were sanger sequenced using Yep13 sequencing primers. B. Quantitative mtDNA inheritance assay validating plasmid 20.4, identified by the screen, and the two candidate genes carried by 20.4. Significance was determined using one-way ANOVA separately on the *HS* (N = 4) and *rho0* (N = 3) crosses with means compared to the vector control and using Dunnett's multiple comparison's test. \*\*\*\* indicates adjusted P value less than 0.0001. All other comparisons were not significantly different. C. Quantitative mtDNA inheritance assay as in b testing high-copy *PET127* on the other isolated *HS* alleles. Significance was determined by student's unpaired T test on the *vector* and high-copy *PET127* pair for each *HS* or *rho0* set (N = 3). \* indicates a P value between less than 0.05. \*\* indicates a P value less than 0.01. \*\*\* indicates a P value between 0.001. All other comparisons were not significantly different.

<https://doi.org/10.1371/journal.pgen.1009808.g003>

suppression are due to features of the mtDNA, not the nuclear DNA of the cells where the *HS* genomes were isolated. From these data we conclude that high-copy *PET127* is a suppressor of a subset of *HS* genomes, and that *PET127* sensitivity depends on the genome but can work on *ORI5* or *ORI2* based *HS* alleles.

### The *Pet127* association with *Rpo41* is responsible for the suppression of *HS ORI5-1*

To gain insights into the molecular mechanism by which high *PET127* levels suppress the preferential inheritance of *HS* mtDNA, we investigated which *Pet127* function contributes to this phenotype. *PET127* is a nuclear-encoded mitochondrial gene that encodes a putative RNA exonuclease that localizes to the mitochondrial inner membrane [46]. *PET127* was discovered as a loss-of-function suppressor of C-terminal *PET122* mutations which block translation of *COX3* mRNA [49], and, while *PET127* deletions fail to cause the petite phenotype implied by the “PET” nomenclature [49], expression of *PET127* from the strong *ADC1* promoter on high-copy plasmids causes loss of mtDNA [46]. *PET127* is homologous to the PD-(D/E)XK exonuclease superfamily [50], and has been proposed to trim the 5' region of mitochondrial mRNAs prior to translation by the mitochondrial ribosome [46,51]. Thus, we first examined whether the 5' RNA exonuclease activity of *PET127* is required for suppression of the *HS* phenotype by mutating four conserved exonuclease active site residues to generate a nuclease-dead allele (*pet127-nd*) [46,49–52]. Deletion of *PET127* increases the size of mitochondrial transcripts, presumably by eliminating the nuclease activity required to trim the transcripts to the normal size [46,52]. To confirm that *pet127-nd* lacks nuclease activity, we performed RNA sequencing and looked for the accumulation of transcripts in regions where the *PET127* wild-type does not usually accumulate (S4 Fig). The RNA sequencing of cells harboring *pet127-nd* showed that the levels of mitochondrial RNA in genic regions was relatively unchanged with respect to *PET127* (S4A Fig), but the intergenic regions and non-coding RNAs showed accumulation of RNA that mimics that of *pet127Δ* (S4B and S4C Fig). These data are consistent with the *pet127-nd* mutant eliminating nuclease activity. Importantly, the *pet127-nd* mutant retained full suppression of *HS* preferential inheritance, as revealed by quantitative mating assay (40% ± 6.7 *rho*<sup>+</sup> colonies) (S5 Fig). Thus, excess RNA exonuclease activity from overexpression of *PET127* does not affect *HS ORI5-1* mtDNA inheritance.

*Pet127* also interacts with the sole mitochondrial RNA polymerase, *Rpo41*, although its role in transcription is unclear [53]. Therefore, we tested whether the association of *Pet127* with *Rpo41* is required for the observed suppression. First, we verified the association between *Pet127* and *Rpo41* by co-immunoprecipitation. As specific antibodies are not available, we created epitope-tagged versions of *PET127* (*PET127-HA*) and *RPO41* (*V5-RPO41*).



Immunoprecipitation of V5-Rpo41 resulted in co-precipitation of Pet127-HA, indicating that these factors interact *in vivo* (Fig 4A).

To identify a *PET127* allele defective in *RPO41* association, we reconstituted the association *in vitro* using recombinant proteins expressed in bacteria. We expressed full length Pet127 lacking its predicted mitochondrial targeting sequence (aa 1–47) and GST-Rpo41 lacking its mitochondrial targeting sequence and performed a pulldown assay in mixed bacterial lysates [53,54]. The mitochondrial targeting sequences are cleaved in the mitochondria and excluded from the mature forms of Pet127 and Rpo41 in yeast. 6xHis-Pet127<sup>48–800</sup> co-precipitated with GST-Rpo41 but not GST alone, indicating a specific and direct interaction between the two proteins (Fig 4B). We then constructed a series of truncation alleles of *PET127* from both the N-terminus and the C-terminus (S6 Fig). The smallest *PET127* allele that bound Rpo41 contained amino acids 48–215 and the largest allele that failed to bind Rpo41 contained amino acids 213–800 (Fig 4B). Thus, amino acids 48–215 of Pet127 are sufficient for binding to Rpo41.

To test whether *PET127* truncations function similarly in yeast, we expressed two of the truncation alleles (including the mitochondrial targeting sequence): *pet127*<sup>Δ48–215</sup>, which lacks the binding region, and *pet127*<sup>1–215</sup> which contains the minimal Rpo41 binding region (Fig 4C). The expression level of both truncated proteins was lower than full-length Pet127 (Fig 4D, Inputs); however, both truncated proteins were imported into mitochondria as they were resistant to proteinase K treatment of a mitochondrial enriched preparation (S7 Fig). Yeast expressing the *pet127*<sup>1–215</sup> allele exhibit a second larger species possibly indicative of uncleaved mitochondrial targeting sequence (Fig 4D). Consistent with this hypothesis, the larger band abundance is reduced by proteinase K degradation (S7 Fig). Co-immunoprecipitation showed that Rpo41 binding with Pet127-nd, the allele lacking the RNA exonuclease activity, was unchanged from wild-type and binding with Pet127<sup>Δ48–215</sup> was less efficient than with Pet127<sup>1–215</sup> (Fig 4D and 4E). Thus, the *PET127* truncation mutants are suitable, in yeast, to interrogate whether Rpo41 binding activity is responsible for high-copy *PET127* suppression of *HS ORI5-1* biased inheritance.

We next used quantitative mating of *HS ORI5-1* and *rho+* yeast carrying multi-copy plasmids with the truncation alleles to test their ability to suppress HS biased inheritance. In spite its relatively low basal protein abundance, overexpression of the *PET127* allele containing the small *RPO41* binding region (*pet127*<sup>1–215</sup>) was sufficient to suppress HS inheritance (23% ± 9.8 *rho+* colonies versus 48% ± 0.44 *rho+* colonies for full-length *PET127*) (Fig 4F). Notably, elimination of the *RPO41* binding region completely abolished *PET127* suppression, as demonstrated by overexpressing the *pet127*<sup>Δ48–215</sup> truncation (1.4% ± 0.73 *rho+* colonies). The suppressive capability of *pet127*<sup>1–215</sup> overexpression is consistent with the observation that plasmid 30.2 isolated from the high copy suppression screen did not contain the full C-terminal region of *PET127* (S3A Fig). These data show that the region of *PET127* that binds to *RPO41* is both necessary and sufficient to suppress HS biased inheritance.

### Reduced mitochondrial transcription suppresses *HS Ori5-1*

We postulated that Pet127 binding to Rpo41 alters the RNA polymerase activity of Rpo41 and that altered mitochondrial RNA polymerase activity affects HS biased inheritance. To test this hypothesis, we asked whether increasing *RPO41* abundance to restore the stoichiometric ratio between Pet127 and Rpo41 amplifies or counteracts the suppressive effect of *PET127* overexpression on HS biased inheritance. We assessed the HS biased inheritance on *rho+* yeast carrying both a high-copy plasmid expressing *V5-RPO41* and a second high-copy plasmid expressing *PET127*. Quantitative mating with *HS ORI5-1* showed that the high-copy *PET127*

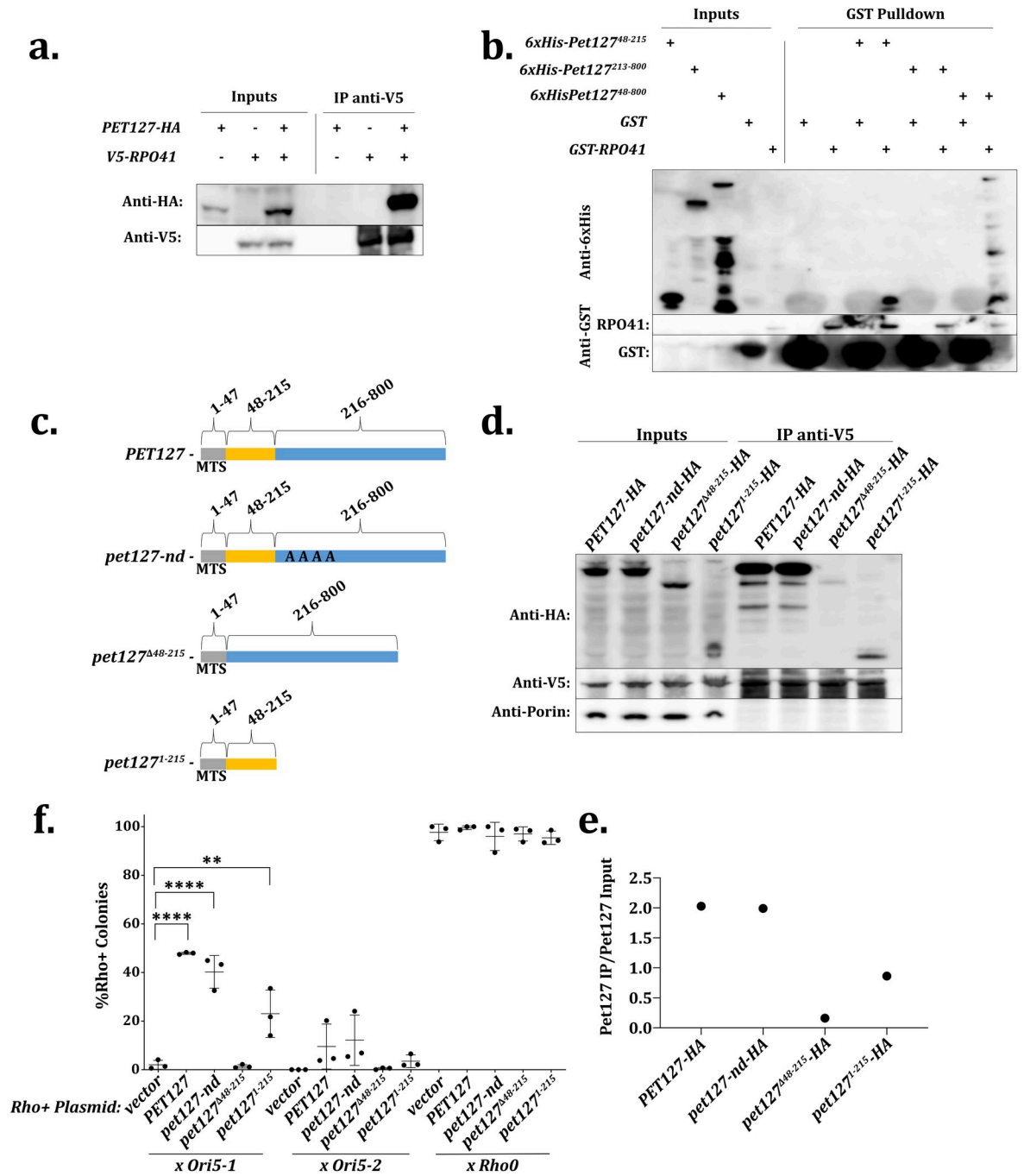


**Fig 4. *PET127* Binds to *RPO41* and the Binding Region is Responsible for Suppression of HS Biased Inheritance. A.** Coimmunoprecipitation of Rpo41 and Pet127. Cells expressing either *PET127-HA*, *V5-RPO41*, or *PET127-HA* and *V5-RPO41* were collected, lysed, and V5-Rpo41 was immunoprecipitated using anti-V5 conjugated beads. Samples were immunoblotted as indicated. **B.** Bacterial expression and lysate mixing of recombinant *RPO41* and *PET127* alleles. The indicated alleles were expressed in BL21 by the addition of IPTG. Cells were collected and lysed in a French press. For IPs, equal amounts of lysate from Pet127 construct expressing cells was mixed with lysate from either GST-Rpo41 or GST only expressing cells and precipitated with glutathione agarose beads. Samples were immunoblotted as indicated. **C.** Diagram of *PET127* alleles. The predicted mitochondrial targeting sequence is amino acids 1–47 in gray [54]. Amino acids 48–215 contain the Rpo41 binding region in yellow, and amino acids 216–800 contain the region lacking Rpo41 binding activity in blue. *pet127-nd* is a nuclease dead allele of *PET127* with amino acids predicted to be conserved active site residues changed to alanines: E346, D378, D391, and K393 [50]. **D.** Co-immunoprecipitation of *PET127-HA* alleles and *V5-RPO41* as in a. Samples were immunoblotted as indicated. Anti-porin used as a negative pulldown control. **E.** Quantitation of IP enrichment in d. **F.** Quantitative mtDNA inheritance assay with *rho+* high copy *PET127* alleles x *HS ORI5-1*, *HS ORI5-2*, or *rho0*. Significance was determined using one-

way ANOVA separately on each *HS* and *rho0* cross with means compared to the vector control using Dunnett's multiple comparison's test ( $N = 3$ ). \*\*\*\* indicates adjusted P-value less than 0.0001 and \*\* indicates an adjusted P-value of 0.0025. All other comparisons were not significantly different.

<https://doi.org/10.1371/journal.pgen.1009808.g004>

plasmid decreased the inheritance of *HS* mtDNA ( $49\% \pm 7.9$  *rho+* colonies) relative to control ( $4.2\% \pm 2.1$  *rho+* colonies) (Fig 5A). In contrast, cells with the high-copy *V5-RPO41* plasmid showed no significant decrease in *rho+* colonies ( $0.55\% \pm 0.62$  *rho+* colonies) relative to control cells (Fig 5A). Interestingly, cells with both *V5-RPO41* and *PET127* high-copy plasmids significantly abolished the suppression effect of the *PET127* plasmid alone ( $6.6\% \pm 0.94$  *rho+* colonies). This finding is consistent with the hypothesis that excess Pet127 binding reduces the polymerase activity of Rpo41. The percent of *rho+* colonies after mating *rho+* strains carrying *V5-RPO41* plasmid or both *V5-RPO41* and *PET127* plasmids to *rho0* cells was not significantly different ( $82\% \pm 10$  in *V5-RPO41*,  $88\% \pm 6.6$  in *PET127 V5-RPO41*) from the strains not carrying the *V5-RPO41* plasmid ( $96\% \pm 2.4$  in strain carrying both empty vectors,  $97\% \pm 1.0$  in *PET127*) (Fig 5A). From these data, we conclude that *RPO41* and *PET127* act in opposition to one another, and, because increasing Pet127 affects HS biased inheritance through Rpo41, there is a strong possibility that Pet127 is an inhibitor of Rpo41 polymerase activity.

As Rpo41 is an RNA polymerase, an increase in Rpo41 abundance should increase mitochondrial transcription, and, if *PET127* is an inhibitor of *RPO41*, increased Pet127 abundance should reduce mitochondrial transcription. Evaluating the mRNA levels of the mitochondrial coding genes *COX3*, *COX2*, and *ATP9* via RT-qPCR showed that, for all loci assessed, the addition of high-copy *V5-RPO41* increases mRNA relative to the control (Figs 5B and S8A). Co-expression of high-copy *PET127* and high-copy *V5-RPO41* greatly reduced the effect of *RPO41*, supporting an inhibitory role for Pet127 in transcription (Figs 5B and S8A). Expression of high-copy *PET127* alone showed a decreasing trend in mRNA levels, with significant effect on *COX3* mRNA, but insignificant effects on *ATP9* and *COX2* (Figs 5B and S8A). None of the tested conditions affected mtDNA levels (S8B Fig).

To further examine the inhibitory role of Pet127, we maximized its effect on transcription by replacing the wild-type promoter on the high-copy *PET127* alleles with the strong galactose-inducible *GAL1/10* promoter. In haploid *rho+* cells carrying the *pGal-PET127* plasmid three hours after galactose addition, *COX3* RNA levels were cut in half by qPCR compared to control strains while mtDNA levels were unaffected (S9A Fig). RNA sequencing performed five hours after galactose addition showed a similar trend for all major mitochondrial gene transcripts relative to the time of galactose addition (S9B Fig). Overall, these data indicate that high level of *PET127* expression causes a general reduction of mitochondrial transcription, supporting the hypothesis that Pet127 is an inhibitor of Rpo41.

In the RNA priming model for mtDNA replication, transcription from the mtDNA *ORI* regions is hypothesized to play a role in DNA replication, raising the possibility that the *PET127* overexpression effect on the HS phenotype is a consequence of altered *ORI* transcription. We therefore monitored *ORI* RNA, utilizing qPCR primers which amplify a transcript, which corresponds to a common area in all "transcription active" *ORIs* (2, 3, 5, ~230bp) as well as a hypothetical-long transcript, common to *ORII* and *ORI6* (~250bp). Surprisingly, *ORI* RNA levels were increased upon *pGAL-PET127* expression in the *rho+* background and the *HS ORI5-1* background (S9C and S9D Fig). However, this increase was independent of Pet127 binding to Rpo41 as the *pGal-pet127<sup>A48-215</sup>* truncation mutant had the same effect as wild-type *PET127* (S9C Fig). Expression of the nuclease dead mutant caused *ORI* RNA to increase above that of the *pGal-PET127* allele which suggests that the nuclease activity affects the abundance of *ORI* transcripts. From these data, we conclude that the levels of the 230 or 250 bp-long *ORI*

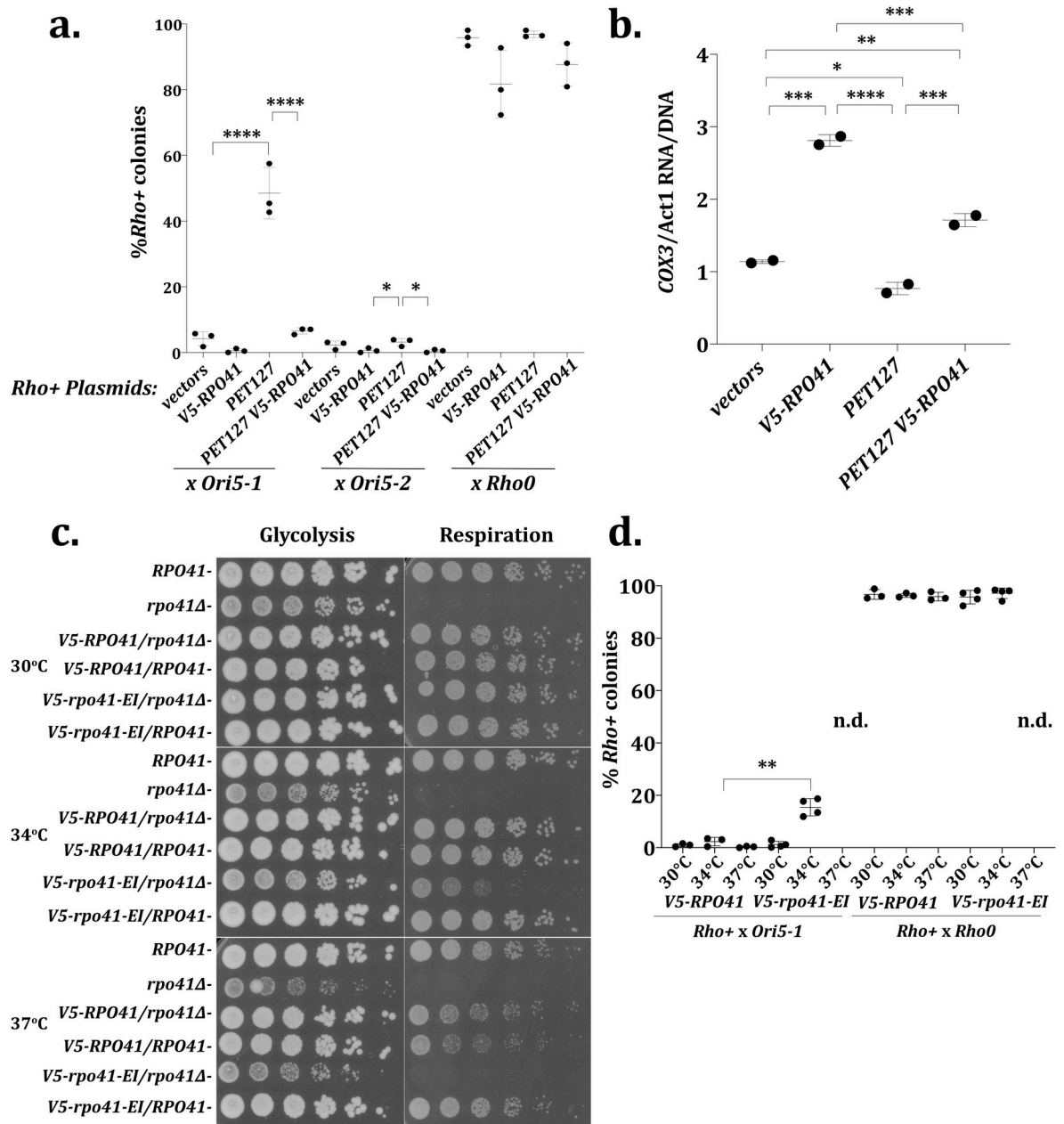


**Fig 5. Reduction of Transcription from the Mitochondrial RNA pol, RPO41, Suppresses HS Biased Inheritance.** A. Quantitative mtDNA inheritance assay on strains carrying all combinations of high-copy *PET127*, high-copy *V5-RPO41*, and their respective empty vector controls. Significance was determined using one-way ANOVA separately on each *HS* and *rho0* cross with means compared to all other samples and using Tukey's multiple comparison's test (N = 3). \*\*\*\* indicates adjusted P value less than 0.0001. \* indicates adjusted P-value less than 0.05. All other comparisons were not significantly different. B. RT-qPCR of *COX3/ACT1* RNA divided by qPCR of *COX3/ACT1* DNA on the high-copy *PET127* high-copy *V5-RPO41* combination strains collected at high cell density to increase respiration. Significance was determined using one-way ANOVA comparing all values with each other using Tukey's multiple comparison's test (N = 2). \*\*\*\* indicates adjusted P-value less than 0.0001, \*\*\* indicates an adjusted P-value of 0.0008 to 0.0001, \*\* indicates an adjusted P-value of 0.0057, \* indicates an adjusted P-value of 0.0275. C. Five-fold serial dilution of strains containing *RPO41* alleles beginning at 1.1 x 10<sup>7</sup> cells/ml plated on glycolysis (YEPD) or respiration (YEPG) utilizing media. Plates were incubated at either 30°C or 34°C for 2 days or 37°C for 3 days. D. Quantitative mtDNA inheritance assay of *rho+* *V5-RPO41* x either *HS ORI5-1* or *rho0 V5-RPO41* and *rho+* *v5-rpo41-EI* x either *HS ORI5-1* or *rho0 v5-rpo41-EI* at 30°C, 34°C, and 37°C. *v5-rpo41-EI* cross at 37°C was not determined as there was synthetic lethality on the diploid selection plates (see S11 Fig). Significance was determined using student's T-test on each temperature between *V5-RPO41* and *v5-rpo41-EI* in *HS* (N = 4) and *rho0* (N = 3) cross. \*\* indicates a P-value of 0.0015. All other comparisons were not significantly different.

<https://doi.org/10.1371/journal.pgen.1009808.g005>

transcripts do not play a role in *PET127* suppression, but that *PET127* expression and nuclease activity can affect levels of those transcripts.

As Pet127 is an inhibitor of Rpo41 when overexpressed, we wanted to know if there are conditions where Pet127 levels change relative to Rpo41 and their inhibitory relationship might be important for cellular life. When *Saccharomyces cerevisiae* undergo fermentation, a fermentable carbon source such as glucose gets converted into the respiratory carbon source ethanol [55]. In batch cultures, the fermentable carbon source is used up as cell density increases [56]. *Saccharomyces cerevisiae* can then utilize the ethanol as a carbon source, and this transition is called diauxic shift [57]. As Rpo41 activity is necessary for respiration, we decided to track Pet127 and Rpo41 protein levels as cells undergo diauxic shift. We found that as cell density increases and diauxic shift occurs Pet127 levels decrease relative to Rpo41 (S10A Fig). Conversely, diluting high density cultures into glucose medium increases Pet127 levels relative to Rpo41 (S10A Fig). We wondered whether the observed decrease was specific to ethanol conditions or whether other respiratory carbon sources cause the same effect. To test this, we grew cells in glucose and then split the culture four ways into medium containing either glucose or the respiratory carbon sources glycerol, acetate, or ethanol and waited to let the cells acclimate to the new conditions. We found that while Rpo41 levels remained the same, Pet127 protein levels decreased in all respiratory conditions (S10B Fig). From these data, we conclude that Pet127 protein levels decrease relative to Rpo41 in respiratory conditions.

To directly assess whether biased inheritance of HS can be prevented by inhibiting Rpo41-mediated mitochondrial transcription we attempted to reduce but not eliminate Rpo41 activity in the course of *rho+* and *HS* mating. Since *rho+* mtDNA is unstable in the *rpo41Δ* background [58], we utilized a temperature sensitive allele of *RPO41*, *v5-rpo41-EI* [53], at a semi-permissive temperature to assess HS preferential inheritance with a partially functional RNA polymerase. We tested the temperature sensitivity of *v5-rpo41-EI* at 30°C, 34°C, and 37°C by testing the viability of serial dilutions of exponentially growing yeast in conditions either requiring respiration for growth or allowing for growth using glycolysis (Fig 5C). The *v5-rpo41-EI* allele permitted haploid cells to grow normally in respiration conditions at 30°C, similar to wild type *RPO41*, but eliminated growth at 37°C, mimicking *rpo41Δ*, and caused an intermediate reduction of growth at 34°C (Fig 5C).

Quantitative mating of *HS ORI5-1* and *rho+* at 37°C, in the *V5-RPO41* background showed no changes relative to the other temperatures (0.31% ± 0.29 *rho+* colonies), but the *v5-rpo41-EI* background showed a reduction of diploid colonies on synthetic dropout plates at 37°C despite being a non-respiratory growth condition (S11 Fig). Because the result would be distorted by the synthetic lethal effect present on the diploid selection plate, we did not assess the percent of *rho+* colonies in the *v5-rpo41-EI* at 37°C when mated with either *HS ORI5-1* or *rho0*. However, quantitative mating of *HS ORI5-1* and *rho+* at 34°C resulted in a small but significant increase in *rho+* colonies in the *v5-rpo41-EI* background (15% ± 3.3) over the *V5-RPO41* background (2.3% ± 1.7 *rho+* colonies) (Fig 5D). No change was observed when mating *rho+* and *HS ORI5-1* at 30°C in either the *V5-RPO41* background (1.0% ± 0.59) or the *v5-rpo41-EI* background (1.2% ± 1.2). As partial reduction of mitochondrial RNA polymerase activity is sufficient to suppress the preferential inheritance of *HS* mtDNA, we conclude that transcription of mitochondrial RNA promotes the *HS ORI5-1* preferential inheritance over *rho+* mtDNA.

## Discussion

### *HS ORI5-1* mtDNA damages *rho+* mtDNA

The main hypothesis regarding the mechanism of HS biased inheritance is that the HS mtDNA is better replicated and outcompetes the *rho+* mtDNA. However, we show here that

during *HS ORI5-1* takeover mtDNA of some regions of *rho+* mtDNA are eliminated while other regions remain. If purely a replication competition was responsible for the HS takeover, a uniform loss of the entire *rho+* genome would be expected rather than loss of some regions before others. Therefore, the introduction of *HS ORI5-1* mtDNA actively eliminates regions of the *rho+* genome. The idea that HS biased inheritance is not exclusively due to replicative advantage is consistent with the observation that there is no correlation between replication rates of different partially suppressive *rho-* mtDNAs and the extent to which they take over the *rho+* mtDNA [41].

How does *HS ORI5-1* mtDNA cause selective elimination of *rho+* mtDNA? HS mtDNA could cause a defect in *rho+* replication. Replication defects that could cause selective genome loss include a subset of origins failing or elongation defects preventing complete genome replication. Alternatively, *HS* mtDNA could directly recombine with *rho+* mtDNA with unequal crossovers causing destruction of *rho+* regions. A recombination DNA destruction mechanism provides an alternative explanation, besides recombination-based replicative-advantage, as to why recombination mutants are reported to reduce HS biased inheritance [39,40].

The HS phenotype damaging *rho+* mtDNA is a harmonious solution to some of the problems of the replicative-advantage model. The replicative advantage model has problems accounting for how there are so few *rho+* cell progeny from a HS cross. The replication advantage model proposes that the replication rate of HS genomes is so superior that almost no progeny obtain *rho+* mtDNA. The *rho+* containing parents then die due to replicative aging. It is known that *rho+* mtDNA is present in the progeny of the first division of a zygote [44]. Once it is inherited to cells, the *rho+* mtDNA would quickly become a pure population [59]. However, according to the DNA damage model, *rho+* mtDNA would have DNA damage which allows it to appear in progeny without a respiration phenotype.

### **Pet127 is a negative regulator of Rpo41**

Although, we show that Pet127 binds and represses Rpo41 function, the molecular mechanism is still unclear. Pet127 binding could be blocking a region required for Rpo41 binding with DNA. Alternatively, Pet127 binding could cause a conformational change in Rpo41 rendering it unable to transcribe RNA or bind to DNA. It is unclear how cells utilize the inhibitory relationship of Pet127 with Rpo41. Pet127 inhibition of Rpo41 could have a buffering role on Rpo41 to allow the cell to respond to fluctuations of Rpo41 levels. Rpo41 activity may be required more in respiratory conditions and Pet127 protein levels dropping in respiratory conditions may be a way cells can regulate Rpo41 activity.

### **Biased inheritance of *ORI5-1* hypersuppressive mtDNA utilizes mitochondrial RNA polymerase activity**

We show that transcription is involved in the HS phenotype because modulation of mitochondrial RNA polymerase activity alters the phenotype. Although a role for transcription is clear, the exact mechanism of transcription involvement in HS is not. The theory that mitochondrial RNA is a required intermediate in HS biased inheritance was previously tested by assessing HS biased inheritance in the *rpo41Δ* background lacking mtRNA [38]. Since *rho+* mtDNA is unstable in the *rpo41Δ* background, a non-preferentially inherited “neutral” *rho-* mtDNA was used in place of *rho+*. These studies showed that HS mtDNA was preferentially inherited over neutral *rho-* mtDNA in *rpo41Δ* cells. The problem with this experiment is that neutral *rho-* mtDNA is not an appropriate substitute for *rho+* mtDNA, as *rho+* mtDNA is inherited far better and has a different transcriptional landscape than the neutral *rho-* mtDNA. By utilizing the temperature sensitive *v5-rpo41-EI* allele at semi-permissive temperatures, we were able to

maintain the stability of *rho+* mtDNA while reducing mitochondrial transcription and show that mitochondrial RNA polymerase, *RPO41*, plays a role in HS biased inheritance.

How mitochondrial RNA plays a role in HS biased inheritance remains unclear. Prior thinking is that the only transcript in HS alleles is *ORI* RNA, so transcription must be involved in the HS phenotype through production of *ORI* RNA. However, we show here that changes in *ORI* RNA levels do not correlate with changes in HS phenotype across *PET127* alleles. Although this finding does not completely rule out a role for *ORI* RNA in the HS phenotype, it is unlikely that *PET127* overexpression reverses HS biased inheritance through *ORI* RNA effects. Instead, we show that reduction of the HS phenotype occurs in concert with a general reduction of *rho+* transcription. How *rho+* transcription could be involved in the HS phenotype has not previously been considered. It is possible that a specific *rho+* transcript or gene product promotes HS biased inheritance. Alternatively, general *rho+* transcription or translation could be required. Given the lack of effects on the *ORI* transcript, it is unclear which specific transcripts are candidates and how, mechanistically, they would impact inheritance.

There are several possible models for how general transcription reduction could reduce biased inheritance. One possibility is that transcription machinery physically blocks *rho+* replication on the same stretch of DNA. If so, then removing RNA polymerase from the genome allows replication machinery access. While it has been shown that transcription can block nuclear replication initiation [60] and replication fork progression [61], it is unclear which, if either, method is responsible for preventing *rho+* replication.

Alternatively, a general reduction of transcription could increase the pool of available ribonucleotides. Hyperactivating RNR pathway, which increases nucleotide availability, partially suppresses HS biased inheritance, indicating that nucleotides are limiting for *rho+* mtDNA during HS takeover [42]. It is thought that ribonucleotides can substitute for deoxyribonucleotides in the yeast mtDNA during replication because of a promiscuous mtDNA polymerase and an absence of a mitochondrial ribonucleotide excision repair pathway [62]. Thus, reducing *rho+* mitochondrial mRNAs could increase the local ribonucleotide pool allowing for elongation utilizing ribonucleotides in a deoxyribonucleotide limited state.

It is puzzling that the methods of HS suppression described here only work on certain HS alleles and not on others. The implication is that the different alleles use different mechanisms for biased inheritance. It could be that the base repeat length of the HS allele determines the method of biased inheritance or that spontaneous mutations in the repeat sequence change the way HS alleles behave.

## Materials and methods

### Yeast strains and culture conditions

All strains are derivatives of W303 (AA2587) unless noted otherwise. See [Table 1](#) for details. Liquid cultures were grown in YEPD (1% yeast extract, 2% peptone, 2% glucose) with additional adenine (55 µg/L), uracil (22.4 µg/L), and tryptophan (80 µg/L) or SD media [2% glucose, 6.7 g/L yeast nitrogen base w/o amino acids (Difco), 2 g/L complete supplement mixture (without Histidine, without Leucine or without Uracil and Leucine, CSM MP Biomedicals)], to maintain plasmid selection, overnight at room temp (~23°C for *rho+* strains) or 30°C (for *rho-0* strains) and diluted back to  $3.3 \times 10^6$  cells/ml and grown at 30°C.

For galactose induction, strains were cultured overnight in SD-Histidine medium (*rho+* strains) or YEP medium (HS strains) with 2% raffinose instead of 2% glucose. Cells were diluted back to  $3.3 \times 10^6$  cells/ml in the same medium, allowed to grow one doubling, and the expression of the galactose promoter was induced by the addition of 1% galactose.

Table 1. List of Yeast Strains Used in this Study.

Strain Number	Relevant Genotype	Fig
AA36030	<i>MATalpha, ade2-1, leu2-3, ura3, trp1-1, HIS3+, can1-100 rho+</i>	S1a
AA41772	<i>MATalpha, ade2-1, leu2-3, ura3, trp1-1, HIS3+, can1-100 HS Rho- HS1a</i>	S1c
AA41773	<i>MATalpha, ade2-1, leu2-3, ura3, trp1-1, HIS3+, can1-100 HS1b HS OR15-1</i>	1, 2, 3b, 3c, 4f, 5a, S1c, S2, S3b S5, S9d
AA41774	<i>MATalpha, ade2-1, leu2-3, ura3, trp1-1, HIS3+, can1-100 HS Rho- HS1c</i>	S1c
AA41775	<i>MATalpha, ade2-1, leu2-3, ura3, trp1-1, HIS3+, can1-100 HS Rho- HS2a</i>	S1c
AA41776	<i>MATalpha, ade2-1, leu2-3, ura3, trp1-1, HIS3+, can1-100 HS Rho- HS2b</i>	3c, S1c
AA41777	<i>MATalpha, ade2-1, leu2-3, ura3, trp1-1, HIS3+, can1-100 HS Rho- HS2c</i>	S1c
AA41778	<i>MATalpha, ade2-1, leu2-3, ura3, trp1-1, HIS3+, can1-100 HS Rho- HS3a</i>	S1c
AA41779	<i>MATalpha, ade2-1, leu2-3, ura3, trp1-1, HIS3+, can1-100 HS3b HS OR15-2</i>	1, 3c, 4f, 5a, S1c, S3b, S5, S9d
AA41780	<i>MATalpha, ade2-1, leu2-3, ura3, trp1-1, HIS3+, can1-100 HS Rho- HS3c</i>	S1c
AA41781	<i>MATalpha, ade2-1, leu2-3, ura3, trp1-1, HIS3+, can1-100 HS Rho- HS4a</i>	S1c
AA41782	<i>MATalpha, ade2-1, leu2-3, ura3, trp1-1, HIS3+, can1-100 HS Rho- HS4b</i>	3c, S1c
AA41783	<i>MATalpha, ade2-1, leu2-3, ura3, trp1-1, HIS3+, can1-100 HS Rho- HS4c</i>	S1c
AA41784	<i>MATalpha, ade2-1, leu2-3, ura3, trp1-1, HIS3+, can1-100 HS Rho- HS5a</i>	S1c
AA41785	<i>MATalpha, ade2-1, leu2-3, ura3, trp1-1, HIS3+, can1-100 HS Rho- HS5b</i>	3c, S1c
AA41786	<i>MATalpha, ade2-1, leu2-3, ura3, trp1-1, HIS3+, can1-100 HS Rho- HS5c</i>	S1c
AA41787	<i>MATalpha, ade2-1, leu2-3, ura3, trp1-1, HIS3+, can1-100 HS6a HS OR13-1</i>	1, 3c, S1c
AA41788	<i>MATalpha, ade2-1, leu2-3, ura3, trp1-1, HIS3+, can1-100 HS Rho- HS6b</i>	S1c
AA41789	<i>MATalpha, ade2-1, leu2-3, ura3, trp1-1, HIS3+, can1-100 HS6c rho0</i>	2, 3b, 3c, 4f, 5a, S1c, S3b S5
AA41790	<i>MATalpha, ade2-1, leu2-3, ura3, trp1-1, HIS3+, can1-100 HS Rho- HS7a</i>	S1c
AA41791	<i>MATalpha, ade2-1, leu2-3, ura3, trp1-1, HIS3+, can1-100 HS Rho- HS7b</i>	3c, S1c
AA41792	<i>MATalpha, ade2-1, leu2-3, ura3, trp1-1, HIS3+, can1-100 HS Rho- HS7c</i>	S1c
AA41793	<i>MATalpha, ade2-1, leu2-3, ura3, trp1-1, HIS3+, can1-100 HS Rho- HS8a</i>	S1c
AA41794	<i>MATalpha, ade2-1, leu2-3, ura3, trp1-1, HIS3+, can1-100 HS Rho- HS8b</i>	3c, S1c
AA41795	<i>MATalpha, ade2-1, leu2-3, ura3, trp1-1, HIS3+, can1-100 HS Rho- HS8c</i>	S1c
AA41796	<i>MATalpha, ade2-1, leu2-3, ura3, trp1-1, HIS3+, can1-100 HS Rho- HS9a</i>	S1c
AA41797	<i>MATalpha, ade2-1, leu2-3, ura3, trp1-1, HIS3+, can1-100 HS Rho- HS9b</i>	3c, S1c
AA41798	<i>MATalpha, ade2-1, leu2-3, ura3, trp1-1, HIS3+, can1-100 HS Rho- HS9c</i>	S1c
AA41799	<i>MATalpha, ade2-1, leu2-3, ura3, trp1-1, HIS3+, can1-100 HS Rho- HS10a</i>	S1c
AA41800	<i>MATalpha, ade2-1, leu2-3, ura3, trp1-1, HIS3+, can1-100 HS Rho- HS10b</i>	3c, S1c
AA41801	<i>MATalpha, ade2-1, leu2-3, ura3, trp1-1, HIS3+, can1-100 HS Rho- HS10c</i>	S1c
AA41802	<i>MATalpha, ade2-1, leu2-3, ura3, trp1-1, HIS3+, can1-100 HS Rho- HS11a</i>	S1c
AA41803	<i>MATalpha, ade2-1, leu2-3, ura3, trp1-1, HIS3+, can1-100 HS11b HS OR12-1</i>	1, 3c, S1c
AA41804	<i>MATalpha, ade2-1, leu2-3, ura3, trp1-1, HIS3+, can1-100 HS Rho- HS11c</i>	S1c
AA41805	<i>MATa, ade2-1, leu2-3, ura3, trp1-1, his3-11,15, can1-100, YEP13-20.4</i>	S3a
AA41806	<i>MATa, ade2-1, leu2-3, ura3, trp1-1, his3-11,15, can1-100, YEP13-30.2</i>	S3a
AA41807	<i>MATa, ade2-1, leu2-3, ura3, trp1-1, his3-11,15, can1-100, YEP13-39.1</i>	S3a
AA41808	<i>MATa, ade2-1, leu2-3, ura3, trp1-1, his3-11,15, can1-100, YEP13-39.4</i>	S3a
AA39745	<i>MATa, ade2-1, leu2-3, ura3, trp1-1, his3-11,15, can1-100, YEP13</i>	2, 3b, 3c, 4f, S2, S3b, S5

(Continued)



Table 1. (Continued)

Strain Number	Relevant Genotype	Fig
AA41322	<i>MATa, ade2-1, leu2-3, ura3, trp1-1, his3-11,15, can1-100, YEP13-20.4b</i> (subclone of AA41805)	3b
AA39746	<i>MATa, ade2-1, leu2-3, ura3, trp1-1, his3-11,15, can1-100, YEP13-PET127</i>	3b, 3c, 4f, S3b
AA41323	<i>MATa, ade2-1, leu2-3, ura3, trp1-1, his3-11,15, can1-100, YEP13-ERP4</i>	3b
AA39257	<i>MATalpha, ura3-52, lys2-801, ade2-101, his3Del200, trp1Del63, leu2Del1, cyh2, kar1Del15, rho0</i>	Materials and Methods
AA39508	<i>MATa, ade2-1, leu2-3, ura3, trp1-1, HIS3+, can1-100, HS OR15-1 rho-</i>	S3c
AA40153	<i>MATa, ade2-1, leu2-3, ura3, trp1-1, HIS3+, can1-100, HS OR15-2 rho-</i>	S3c
AA38266	<i>MATa, ade2-1, leu2-3, ura3, trp1-1, HIS3+, can1-100, rho0</i>	S3c
AA39535	<i>MATalpha, ade2-1, leu2-3, ura3, trp1-1, his3-11,15, can1-100, YEP13</i>	S3c
AA39534	<i>MATalpha, ade2-1, leu2-3, ura3, trp1-1, his3-11,15, can1-100, YEP13-PET127</i>	S3c
AA39500	<i>MATa, ade2-1, leu2-3, ura3, trp1-1, his3-11,15, can1-100, PET127-6xHA::KANmx6</i>	4a
AA39479	<i>MATa, ade2-1, leu2-3, trp1-1, his3-11,15, can1-100, ura3::RPO41preseq-3xV5-RPO41::URA3, rpo41::KANmx6</i>	4a
AA39607	<i>MATa, ade2-1, leu2-3, trp1-1, his3-11,15, can1-100, ura3::RPO41preseq-3xV5-RPO41::URA3, rpo41::KANmx6, PET127-6xHA::KANmx6</i>	4a, 4d, 4e, S10a, S10b
AA2587	<i>MATa, ade2-1, leu2-3, ura3, trp1-1, his3-11,15, can1-100</i>	1, S4a, S4b, S4c
AA39672	<i>MATa, ade2-1, ura3, trp1-1, his3-11,15, can1-100, LEU2::pet127-nd</i>	S4a, S4b, S4c
AA39670	<i>MATa, ade2-1, ura3, trp1-1, his3-11,15, can1-100, pet127::KANmx6, LEU2::pet127-nd</i>	S4a, S4b, S4c
AA38088	<i>MATa, ade2-1, leu2-3, ura3, trp1-1, his3-11,15, can1-100, pet127::KANmx6</i>	S4a, S4b, S4c
AA40696	<i>MATa, ade2-1, leu2-3, trp1-1, his3-11,15, can1-100, pet127-nd-6xHA::HIS3, ura3::RPO41preseq-3xV5-RPO41::URA3, rpo41::KANmx6</i>	4d, 4e
AA40684	<i>MATa, ade2-1, leu2-3, trp1-1, his3-11,15, can1-100, ura3::RPO41preseq-3xV5-RPO41::URA3, rpo41::KANmx6, pet127(1-215)-6xHA::HIS3</i>	4d, 4e
AA40694	<i>MATa, ade2-1, leu2-3, trp1-1, his3-11,15, can1-100, pet127(Δ48-215)-6xHA::HIS3, ura3::RPO41preseq-3xV5-RPO41::URA3, rpo41::KANmx6</i>	4d, 4e
AA40287	<i>MATa, ade2-1, leu2-3, trp1-1, his3-11,15, can1-100, ura3, Yep13-pet127(Δ48-215)</i>	4f
AA40316	<i>MATa, ade2-1, leu2-3, trp1-1, his3-11,15, can1-100, ura3, Yep13-pet127(1-215)</i>	4f
AA39617	<i>MATa, ade2-1, leu2-3, trp1-1, his3-11,15, can1-100, ura3, Yep13-pet127-nd</i>	4f
AA40317	<i>MATa, ade2-1, leu2-3, ura3, trp1-1, his3-11,15, can1-100, YEP13, pRS426</i>	5a, 5b, S8a, S8b
AA40319	<i>MATa, ade2-1, leu2-3, ura3, trp1-1, his3-11,15, can1-100, YEP13-PET127, pRS426</i>	5a, 5b, S8a, S8b
AA40318	<i>MATa, ade2-1, leu2-3, ura3, trp1-1, his3-11,15, can1-100, YEP13, pRS426-MTS-3xV5-RPO41</i>	5a, 5b, S8a, S8b
AA40320	<i>MATa, ade2-1, leu2-3, ura3, trp1-1, his3-11,15, can1-100, YEP13-PET127, pRS426-MTS-3xV5-RPO41</i>	5a, 5b, S8a, S8b
AA36029	<i>MATa, ade2-1, leu2-3, ura3, trp1-1, HIS3+, can1-100</i>	5c, S11
AA40931	<i>MATa, ade2-1, leu2-3, ura3, trp1-1, can1-100, rpo41::KANmx6, Rho0</i>	5c, S11
AA40974	<i>MATa, ade2-1, trp1-1, leu2-3, can1-100, ura3::RPO41preseq-3xV5-RPO41::URA3, HIS3+</i>	5c, S11
AA40937	<i>MATa, ade2-1, trp1-1, his3-11,15, can1-100, ura3::RPO41preseq-3xV5-RPO41::URA3, rpo41::KANmx6, HIS+</i>	5c, S11

(Continued)

Table 1. (Continued)

Strain Number	Relevant Genotype	Fig
AA40972	<i>MATa, ade2-1, trp1-1, leu2-3, can1-100, ura3::RPO41preseq-3xV5-RPO41-EI::URA3, HIS3+</i>	5c, S11
AA40966	<i>MATa, ade2-1, trp1-1, leu2-3, can1-100, ura3::RPO41preseq-3xV5-RPO41-EI::URA3, rpo41::KANmx6, HIS3+</i>	5c, S11
AA41033	<i>MATa, ade2-1, trp1-1, his3-11,15, can1-100, ura3::RPO41preseq-3xV5-RPO41::URA3, rpo41::KANmx6, LEU2+, Rho- (ORI5-1)</i>	5d
AA41017	<i>MATa, ade2-1, trp1-1, his3-11,15, can1-100, ura3::RPO41preseq-3xV5-RPO41-EI::URA3, rpo41::KANmx6, LEU2+, Rho- (ORI5-1)</i>	5d
AA40982	<i>MATa, ade2-1, trp1-1, his3-11,15, can1-100, ura3::RPO41preseq-3xV5-RPO41::URA3, rpo41::KANmx6, LEU2+, Rho0</i>	5d S1c
AA41006	<i>MATa, ade2-1, trp1-1, his3-11,15, can1-100, ura3::RPO41preseq-3xV5-RPO41-EI::URA3, rpo41::KANmx6, LEU2+, Rho0</i>	5d
AA40938	<i>MATalpha, ade2-1, trp1-1, his3-11,15, can1-100, ura3::RPO41preseq-3xV5-RPO41::URA3, rpo41::KANmx6, HIS+</i>	5d, S1c
AA40967	<i>MATalpha, ade2-1, trp1-1, leu2-3, can1-100, ura3::RPO41preseq-3xV5-RPO41-EI::URA3, rpo41::KANmx6, HIS3+</i>	5d
AA41640	<i>MATa, ade2-1, leu2-3, trp1-1, his3-11,15, can1-100, Pet127-6xHA::HIS3, TOM70-GFP::KanMX</i>	S7
AA41642	<i>MATa, ade2-1, leu2-3, trp1-1, his3-11,15, can1-100, Pet127(Δ48–215)-6xHA::HIS3, TOM70-GFP::KanMX</i>	S7
AA41643	<i>MATa, ade2-1, leu2-3, trp1-1, his3-11,15, can1-100, Pet127(1–215)-6xHA::HIS3, TOM70-GFP::KanMX</i>	S7
AA41809	<i>MATa, ade2-1, leu2-3, trp1-1, his3-11,15, can1-100, ura3, pYX223-mtGFP</i>	S9a, S9b
AA39631	<i>MATa, ade2-1, leu2-3, trp1-1, his3-11,15, can1-100, ura3, pRS423</i>	S9a, S9b, S9c
AA39838	<i>MATa, ade2-1, leu2-3, trp1-1, his3-11,15, can1-100, ura3, pRS423-pGal-PET127-3xV5</i>	S9a, S9b, S9c
AA40159	<i>MATa, ade2-1, leu2-3, trp1-1, his3-11,15, can1-100, ura3, pRS423-pGal-pet127-nd-3xV5</i>	S9a, S9b, S9c
AA40237	<i>MATa, ade2-1, leu2-3, trp1-1, his3-11,15, can1-100, ura3, pRS423-pGal-pet127Δ(48–215)-3xV5</i>	S9a, S9b, S9c
AA40335	<i>MATa, ade2-1, leu2-3, trp1-1, his3-11,15, can1-100, ura3, pRS423-pGal-pet127(1–215)-3xV5</i>	S9a, S9b, S9c
AA41810	<i>MATalpha, ade2-1, leu2-3, ura3, HIS3+, can1-100, trp1-1 LEU2::pGal1-PET127 (Single copy integration) HS ORI5-1 rho-</i>	S9d
AA41811	<i>MATalpha, ade2-1, leu2-3, ura3, HIS3+, can1-100, trp1-1 LEU2::pGal1-PET127 (Single copy integration) HS ORI5-2 rho-</i>	S9d

<https://doi.org/10.1371/journal.pgen.1009808.t001>

### EtBr Treatment (Generation of *rho0* and *HS rho-*)

For generation of *rho0* cells of a particular strain, cells were grown in YEPD + 10μg/ml ethidium bromide for 3 days, diluted back each morning. After treatment cells were streaked to single colonies and lack of mtDNA was confirmed via DAPI staining at 2μg/ml. Generation of *HS* alleles was performed by growing log phase *rho+* cells in 5μg/ml EtBr for 100 minutes and plated on YEPD plates to ~200 cells per plate.

### Screen

*Rho+* cells were transformed with Yep13 high-copy library [45] and were plated on plasmid selection media. Colony plates were replica plated to lawns of *HS ORI5-1*, and further replica plated to diploid selection medium and replica plated again to YEPD with no additional

adenine. Identified colonies were selected from the initial transformation plate and the assay was repeated on those colonies. Plasmids from colonies which scored both times were Sanger sequenced using Yep13 sequencing primers. The resulting sequences were identified via NCBI blast [63].

### Cytoduction

HS strains were transformed with a *matA* cassette and a Pringle deletion cassette for *matAlpha* and mated with *rho0* karyogomy defective mtDNA shuttling strain AA39257 and plated on YEPD + 10 $\mu$ g/ml Cycloheximide to select for homozygous *cyh2 $\Delta$*  present only in haploid AA39257. The resulting colonies were screened for cells containing mtDNA via DAPI indicating transfer of HS mtDNA from the HS strain to the AA39257 parent. The resulting cells were mated with *rho0* recipient strains, and plated on SD-Arg+ 50mg/ml Canavanine to select for homozygous *can1-1* allele present only in the haploid recipient strains. The resulting colonies were checked for mtDNA by staining with 2 $\mu$ g/ml DAPI and confirmed to be haploid by mating complementation on minimal media.

### Mating assay and temperature shifts

Log phase growing cells were mated by mixing  $2.2 \times 10^7$  cells from each parent into 1ml YEPD at room temperature for 5 hours. Cells were diluted 1:1000 and plated on diploid selection plates (SD-His-Leu or SD-His-Ura-Leu) for 48hrs at either 30°C, 34°C, or 37°C and then replica plated to YEPG (1% yeast extract, 2% peptone, 3% glycerol) plates and placed at the same temperature for 72 hours. Percent *rho+* cells was determined by  $100 \times \frac{\text{colonies growing on YEPG}}{\text{colonies growing on diploid selection}}$ . A colony was considered growing if any subregion of the colony was growing.

### Rpo41-V5-EI temperature sensitivity

Mid-log ( $\sim 1.1 \times 10^7$  cells/ml) cultures were diluted to  $1.1 \times 10^7$  cells/ml and five-fold serially diluted 5 times and 4  $\mu$ l was plated on either YEPD, YEPG, or SD-His and placed at either 30°C, 34°C, or 37°C for 2 days.

### Cloning and strain construction

Strains were constructed using standard gene integration or tagging strategies [64]. Plasmids were constructed using standard cloning techniques and described in Table 2 [65].

### DNA isolation

DNA for qPCR and colony PCRs was isolated using a modified smash and grab protocol from [66] with RNase treatment. The mtDNA isolation for SMRT sequencing was done similarly using two phenol chloroform extractions on pellets enriched for mitochondria using the mitochondrial isolation technique below.

### SMRT sequencing

mtDNA isolated as above was sequenced using SMRT sequencing technology on Pacific Biosciences Sequel II [67]. 10kb insert size was selected for on 0.75% agarose Blue Pippin cassettes obtaining 12-13kb mean length inserts and mean read length of 6-7kb. Long reads were computationally divided into 50nt fragments and mapped using BWA-mem onto SGD *sacCer3* genome wildtype reference and viewed on IGV [68].

Table 2. List of Plasmids Used in this Study.

Plasmid Number	Description	Fig
pAA44	YEpl3	2, 3b, 3c, 4f, 5a, 5b, S2, S3b, S3c, S5, S8a, S8b
pAA2582	YEpl3-Erp4	3b
pAA2581	YEpl3-Pet127	3b, 3c, 4f, 5a, 5b, S3b, S3c, S5, S8a, S8b
20.4	YEpl3-[3'RTS1, YOR015W, ERP4, PET127, 5'ROD1]	3b, S3a
30.2	YEpl3-[3'RTS1, YOR015W, ERP4, 5'PET127]	S3a
39.1	YEpl3-[3'CHS1, ARS1414, DUG3, YNL190W, SRP1]	S3a
39.4	YEpl3-[3'SEC27, MRM2, RPL1b, 5'PCL10]	S3a
pAA2758	pGEX-6P-1-V5-Rpo41	4b
pAA2778	pET15b-Pet127-6xHis (Derived from pET15b Novagen (EMD Millipore))	4b
pAA2058	pGEX-6P-1 (Amersham)	4b
pAA2794	pET15b-Pet127-N504-6xHis	4b
pAA2806	pET15b-Pet127-C1764-6xHis	4b
pAA2703	pRS306-Rpo41-internal-3xV5	4a, 4d, 5c, 5d, S10a, S10b, S11
pAA2782	pNH605-Pet127-nd-3xV5	4d, S7
pAA2832	pNH605-Pet127 <sup>Δ48-215</sup> -3xV5	4d, S7
pAA2842	pNH605-Pet127 <sup>1-215</sup> -6xHA-His3	4d, S7
pAA2713	YEpl3-Pet127-nd	4f
pAA2833	YEpl3-Pet127 <sup>Δ48-215</sup>	4f
pAA2835	YEpl3-Pet127 <sup>1-215</sup>	4f
pAA2837	pRS426-RPO41-internal-3xV5	5a, 5b, S8a, S8b
pAA2924	pRS306-Rpo41-EI-internal-3xV5	5c, 5d, S11

<https://doi.org/10.1371/journal.pgen.1009808.t002>

## Colony PCR

Strains were mated as in the quantitative mating assay. Whole individual diploid colonies were scraped off plates and DNA was isolated from them using the DNA isolation protocol. DNA was normalized across samples and added to PCR reactions using the colony PCR primer sets in Table 3. PCRs were run on either 1% or 2% (ATP9) agarose gel made with 1x TAE (40mM Tris base, 20mM Acetic Acid, 1mM EDTA) and 0.1μg/ml EtBr for 25 minutes at 130V constant voltage in 1 x TAE.

Table 3. List of Primers Used in this Study.

Primer Set	Forward Primer	Reverse Primer
Yep13 Backbone	TTCGCTACTTGGAGCCACTAT	ATCGGTGATGTCGGCGATATA
ACT1 qPCR set	GTACCACCATGTTCCCAGGTATT	CAAGATAGAACCACCAATCCAGA
COX3 qPCR set	TCCATTCAGCTATGAGTCCTGA	CTGCGATTAAGGCATGATGA
COX2 qPCR set	GTGGTGAAACTGTTGAATTTGAATC	AGCAGCTGTTACAACGAATCTA
ATP9 qPCR set	ATTGGAGCAGGTATCTCAACAA	GCTTCTGATAAGGCGAAACC
ORI qPCR set	ATAGGGGGAGGGGTGGGTGAT	GGGACCCGGATATCTTCTTGTATTATC
Nuclear Colony PCR Set ( <i>PET127</i> locus)	GCGCGTTCCGTCAATGCC	TTTCAGTAGATTAATCGCCTTGTC
ORI Colony PCR set	ATAGGGGGAGGGGTGGGTGAT	GGGACCCGGATATCTTCTTGTATTATC
COX2 Colony PCR set	CAGCAACACCAATCAAGAAGG	ATGACCTGTCCCACACAAC
COX3 Colony PCR set	GACACATTTAGAAAGAAGTAGACATCAAC	GACTCCTCATCAGTAGAAGACTACG
ATP9 Colony PCR set	ATTGGAGCAGGTATCTCAACAA	GCTTCTGATAAGGCGAAACC
COX1 Nterm Colony PCR set	TAGCTGCACCTGGTTCACAA	CCTCTTTCAGTTGATCCCTCAC
COX1 Cterm Colony PCR set	ACTTTCTTCCCTCCGAATC	CCTGCGATTGTCCATACTT

<https://doi.org/10.1371/journal.pgen.1009808.t003>

## RNA Isolation and qPCR

RNA was isolated from  $4.4 \times 10^7$  cells using acid phenol and purified using an RNeasy kit (Qiagen) with on column DNase treatment (Qiagen). Reverse transcription was performed on 750ng of RNA using SuperScript III First-Strand Synthesis SuperMix (Life Technologies) and qPCR was performed using SYBR Premix Ex Taq (Tli RNaseH Plus) or the equivalent TB Green Premix Ex Taq (Tli RNaseH Plus) from TaKaRa. Signals were normalized to *ACT1* levels and normalized to the control average. Primers are described in [Table 3](#).

## RNA sequencing

Isolated total yeast RNA as above were processed using Ribozero rRNA removal for Yeast (Illumina). For *pet127-nd* RNA profiling, sequencing was performed on NextSeq500 with 75 + 75 bases pair-end run with 6 + 6 nucleotide indexes. Pair end sequencing reads were mapped to sacCer3 reference genome using star/2.5.3a [69]. The regions of interest were defined using the bed file format. The coverage sub-command of bedtools/2.26.0 was applied to calculate the number of sequences mapped to the specific regions of the reference genome using alignment bam files. The counts of all samples were merged to a matrix with each sample per column and each location per row using MIT IGB in house tool. The regions were defined by the boundaries in [Table 4](#) modified from [7].

For the *pGal-PET127* RNA sequencing experiment, sequencing was performed on HiSeq2000 with 40 bases single end run with 8 + 8 nucleotide indexes [70]. Single end sequencing reads were mapped to sacCer3 reference genome using star/2.5.3a. rsem/1.3.0 was applied for gene level counting, fpkm and tpm calculation. The raw counts, fpkm, and tpm values of each gene in all sample were merged into three corresponding matrices using IGB in house tools. The matrices were formatted as each sample per column and each gene per row. Hierarchical clustering was performed using TIBCO Spotfire 7.11.1 based on  $\log_2(\text{fpkm}+1)$  of the expressed coding genes. Differential expression comparisons between 5 hour and 0 hour under different conditions were carried out using Deseq2 1.10.1 under r/3.2.3. with raw counts as input.

## Mitochondria isolation

Mitochondrial enrichment protocol modified from [71]. Cells were grown into logarithmic phase growth, transferred into DTT buffer (0.1 M Tris pH 9.4, 10 mM DTT) to shake for 20 minutes at 30°C, and transferred into zymolyase buffer (1.2M sorbitol, 20mM  $\text{K}_2\text{HPO}_4$  pH 7.4) with the addition of 1% zymolyase 100T or equivalent for 1 hour at 30°C to digest the cell wall. Cells were lysed by dounce homogenization 20 strokes in homogenization buffer (0.6M sorbitol, 10mM Tris pH 7.4, 1mM EDTA, 0.2% BSA no fatty acid, 1mM PMSF). Mitochondria were isolated by differential centrifugation 5 minutes at 1200g, the resulting supernatant was spun for 5 minutes at 2000g, and the resulting supernatant was spun at 17500g for 15 minutes all at 4°C. The resulting pellet was resuspended in SEM buffer (0.25M sucrose, 10mM MOPS KOH pH 7.2, and 1mM EDTA). For assessing whether proteins are mitochondrial, 3µg of enriched mitochondria was treated with 50µg/ml proteinase K for 5mins at 37°C. The reaction was stopped by addition of TCA to 12.5%.

## Coimmunoprecipitation assay

Cells were grown in YEPD to  $1.1 \times 10^7$  cells /ml.  $1.1 \times 10^9$  cells were collected and frozen. Cells were lysed with a FastPrep-24 Classic (MP Biomedicals, Speed 6.5, 60s, 10 cycles) with 200µl NP40 buffer [50mM Tris pH7.5, 150mM NaCl, 1% Np40 (IGEPAL) and Halt Protease Inhibitor Cocktail (Thermo Fisher Scientific)]. Lysates were brought up to 1.5ml with NP40 buffer

**Table 4. Bin Boundaries for *pet127-nd* RNA Sequencing.**

Description	Start	Start
<i>RPM1 to UGG Proline tRNA</i>	1	730
<i>UGG Proline tRNA</i>	731	802
<i>UGG Proline tRNA to ORI1</i>	803	4011
<i>ORI1</i>	4012	4312
<i>ORI1 to 15S rRNA</i>	4313	6545
<i>15S rRNA</i>	6546	8194
<i>15S rRNA to UCA Tryptophan tRNA</i>	8195	9373
<i>UCA tryptophan tRNA</i>	9374	9444
<i>UCA tryptophan tRNA to ORI8</i>	9445	12509
<i>ORI8</i>	12510	12780
<i>ORI8 to COX1</i>	12781	13817
<i>COX1</i>	13818	26701
<i>COX1 to ATP8</i>	26702	27665
<i>ATP8</i>	27666	27812
<i>ATP8 to ATP6</i>	27813	28486
<i>ATP6</i>	28487	29266
<i>ATP6 to ORI7</i>	29267	30219
<i>ORI7</i>	30220	30594
<i>ORI7 to ORI2</i>	30595	32230
<i>ORI2</i>	32231	32501
<i>ORI2 to UUC glutamate tRNA</i>	32502	35372
<i>UUC glutamate tRNA</i>	35373	35444
<i>UUC glutamate tRNA to COB</i>	35445	36539
<i>COB</i>	36540	43647
<i>COB to ORI6</i>	43648	44888
<i>ORI6</i>	44889	45225
<i>ORI6 to ATP9</i>	45226	46722
<i>ATP9</i>	46723	46953
<i>ATP9 to UGA serine tRNA</i>	46954	48200
<i>UGA serine tRNA</i>	48201	48290
<i>UGA serine tRNA to VAR1</i>	48291	48900
<i>VAR1</i>	48901	50097
<i>VAR1 to ORI3</i>	50098	54566
<i>ORI3</i>	54567	54840
<i>ORI3 to ORI4</i>	54841	56566
<i>ORI4</i>	56567	56832
<i>ORI4 to 21S rRNA</i>	56833	58008
<i>21S rRNA</i>	58009	62447
<i>21S rRNA to UGU threonine tRNA</i>	62448	63861
<i>UGU threonine tRNA</i>	63862	63934
<i>UGU threonine to GCA cysteine tRNA</i>	63935	64414
<i>GCA cysteine tRNA</i>	64415	64487
<i>GCA cysteine tRNA to GUG histidine tRNA</i>	64488	64596
<i>GUG histidine tRNA</i>	64597	64667
<i>GUG histidine tRNA to UAA leucine tRNA</i>	64668	66094
<i>UAA leucine tRNA</i>	66095	66176
<i>UAA leucine tRNA to UUG glutamine tRNA</i>	66177	66209

(Continued)

Table 4. (Continued)

Description	Start	Start
<i>UUG glutamine tRNA</i>	66210	66282
<i>UUG glutamine tRNA to UUU lysine tRNA</i>	66283	67060
<i>UUU lysine tRNA</i>	67061	67132
<i>UUU lysine tRNA to UCU arginine tRNA</i>	67133	67308
<i>UCU arginine tRNA</i>	67309	67381
<i>UCU arginine tRNA to UCC glycine tRNA</i>	67382	67467
<i>UCC glycine tRNA</i>	67468	67539
<i>UCC glycine tRNA to GUC aspartate tRNA</i>	67540	68321
<i>GUC aspartate tRNA</i>	68322	68393
<i>GUC aspartate tRNA to GCU Serine tRNA</i>	68394	69202
<i>GCU Serine tRNA</i>	69203	69285
<i>GCU Serine tRNA to ACG arginine tRNA</i>	69286	69288
<i>ACG arginine tRNA</i>	69289	69359
<i>ACG arginine tRNA to UGC alanine tRNA</i>	69360	69845
<i>UGC alanine tRNA</i>	69846	69918
<i>UGC alanine tRNA to GAU Isoleucine tRNA</i>	69919	70161
<i>GAU Isoleucine tRNA</i>	70162	70234
<i>GAU Isoleucine tRNA to GUA tyrosine tRNA</i>	70235	70823
<i>GUA tyrosine tRNA</i>	70824	70908
<i>GUA tyrosine tRNA to GUU Asparagine tRNA</i>	70909	71432
<i>GUU Asparagine tRNA</i>	71433	71504
<i>GUU Asparagine tRNA to CAU methionine tRNA 1</i>	71505	72631
<i>CAU methionine tRNA 1</i>	72632	72705
<i>CAU methionine tRNA 1 to COX2</i>	72706	73757
<i>COX2</i>	73758	74513
<i>COX2 to GAA phenylalanine tRNA</i>	74514	77430
<i>GAA phenylalanine tRNA</i>	77431	77502
<i>GAA phenylalanine tRNA to UAG threonine tRNA</i>	77503	78088
<i>UAG threonine tRNA</i>	78089	78162
<i>UAG threonine tRNA to UAC valine tRNA</i>	78163	78532
<i>UAC valine tRNA</i>	78533	78605
<i>UAC valine tRNA to COX3</i>	78606	79212
<i>COX3</i>	79213	80022
<i>COX3 to ORI5</i>	80023	82328
<i>ORI5</i>	82329	82600
<i>ORI5 to CAU methionine tRNA 2</i>	82601	85034
<i>CAU methionine tRNA 2</i>	85035	85107
<i>CAU methionine tRNA 2 to RPM1</i>	85108	85294
<i>RPM1</i>	85295	85777
<i>RPM1 to UGG Proline tRNA</i>	85778	85779

<https://doi.org/10.1371/journal.pgen.1009808.t004>

and were pelleted by centrifugation at 20,000g for 10 minutes at 4C. 1% of sample was taken for Input and boiled with 10µl of 3x SDS sample buffer, and the rest of the lysates were brought to 0.2% BSA. Clarified sample was added to 20µl of Anti-V5 agarose affinity gel antibody beads (Sigma) and incubated for 2 hours at 4C. Beads were washed 3 times with Np40 buffer with Protease inhibitor and 2 times in NP40 buffer without inhibitors. To elute, 30µl of 1.5x SDS sample buffer was added to the beads and samples were boiled for 5 minutes.

## Immunoblotting

Samples in SDS sample buffer were run on 8% polyacrylamide gels in SDS running buffer (0.1918M glycine, 0.0248M Tris base, 0.1%SDS), or gradient gels in MES running buffer (2.5mM MES, 2.5 mM Tris Base, 0.005% SDS, 0.05mM EDTA pH7.3), transferred to PVDF membranes via semi-dry transfer, washed with PBST (10mM, 2.7mM potassium chloride, 137mM sodium chloride, and 1.76mM potassium phosphate. pH 7.4 + 0.1% Tween-20), blocked with PBST and 3% milk for 1 hour and probed overnight in 1xPBS with 1% milk, 1% BSA, 0.1% Sodium Azide and with one of the following primary antibody dilutions: Mouse Anti-HA (1:2000; HA.11, Biolegend), Mouse Anti-V5 (1:2000; R960-25, Thermo-Fisher Scientific), Mouse Anti-VDAC/Porin (1:1000; 16G9E6BC4/ab110326, Abcam), Mouse Anti-6xHis (1:5000, ab18184, Abcam), Mouse Anti-GST (1:5000, ab19256, Abcam), Mouse Anti-PGK (1:5000; 22C5D8, Thermo-Fisher Scientific), Mouse Anti-COX4 (1:1000; ab110272, Abcam), Mouse Anti-GFP (1:1000; JL-8, Clontech). Ponceau S (Abcam) was applied before blocking for 15 minutes and destained for 30 minutes with distilled water. Blots were washed three times with PBST and probed with secondary antibodies diluted in PBS with 1% milk and 1% BSA for one hour at 4°C. Secondary antibody dilutions were Anti-mouse HRP 1:10,000 and Anti-mouse HRP TrueBlot 1:1000 (for coimmunoprecipitation experiments). Membranes were washed three times in PBST and blots were imaged using the ECL Plus system (GE healthcare).

## Bacterial expression and binding and truncations

BL21 Bacteria containing expression plasmids, described in Table 5, were grown in LB+AMP (1% Difco Bacto Tryptone, 0.5% Difco Yeast Extract, 1% NaCl, 10mM Tris pH 7.5, Amp 0.1 mg/ml) overnight at 37°C. Cells were diluted to  $2.66 \times 10^8$  cells/ml in LB + AMP and grown at 37°C for 1h, IPTG was added to 0.5 mM final concentration and cells were allowed to express for 5h at 37°C. Cells were spun at 22K g for 20 minutes at 4°C and resuspended to  $1.33 \times 10^{10}$  cells/ml in PBS + PI [cOmplete, mini, EDTA-free Protease Inhibitor Cocktail (Millipore-Sigma) 1/50mls] + 0.3% BSA. Cells were lysed via French press. GST expressing samples were added to Glutathione beads (pre-washed in PBS+PI). Beads were incubated for 2h at 4°C and spun down at 500 rcf for 2 minutes at 4°C. Beads were washed 3 times with cold NP40 buffer + PI + BSA 0.3%. Equal amounts of non-GST expressing samples were added to the beads. Beads were incubated for 2h at 4°C and spun down at 500 rcf for 2 minutes at 4°C. Beads were washed 3 times with cold NP40 buffer + PI + BSA 0.3% and washed 2 times with NP40 buffer. Protein was eluted by adding 2x SDS Sample buffer equal in volume to beads and boiling for 5 minutes.

## Diauxic shift experiments

For the glucose to ethanol shift, cells were grown overnight in YEPD medium and diluted back to  $3.3 \times 10^7$  cells/ml in YEPD. Cells were grown for 12 hours with  $2.2 \times 10^7$  cells collected

**Table 5. List of Bacterial Strains Used in this Study.**

Strain number	Relevant Genotype	Fig
AAE568	BL21 pGEX-6P-1-V5-Rpo41 (pAA2758)	4b
AAE569	BL21 pET15b-PET127-6xHis (pAA2778)	4b
AAE570	BL21 pGEX-6P-1 (pAA2058)	4b
AAE571	BL21 pET15b-PET127N504-6xHis (pAA2794)	4b
AAE572	BL21 pET15b-Pet127-C1764-6xHis (pAA2806)	4b

<https://doi.org/10.1371/journal.pgen.1009808.t005>



every 2 hours. For the ethanol to glucose shift, A  $2.2 \times 10^7$  cells from an overnight culture were collected and then the culture was diluted back to  $3.3 \times 10^6$  cells/ml in YEPD.  $2.2 \times 10^7$  cells were collected 3h, 5h, and 7h later.

### Medium swap experiment

Cells were grown overnight in YEPD medium and diluted back to  $1.1 \times 10^7$  cells/ml and grown until  $1.1 \times 10^7$  cells/ml.  $2.2 \times 10^7$  cells were collected and then equal amounts of cells were collected using filters (Supor membrane disc filters, Pall laboratory, 47mm, 0.8 $\mu$ M, VWR) and released into YEPD, YEPG (2% Glycerol), YEPA (1% yeast extract, 2% peptone, 2% Potassium Acetate). YEPE (1% yeast extract, 2% peptone, 2% ethanol) at  $1.1 \times 10^7$  cells/ml. Cells were grown for 4 hours and  $2.2 \times 10^7$  cells were collected and immunoblotted.

### Supporting information

**S1 Fig. Generation of *rho*- and *rho0* Colonies over Time upon Addition of EtBr.** A. 5  $\mu$ g/ml EtBr was added to *rho*+ cells and cells were collected every 30 minutes for 180 minutes. Colonies were assessed for respiration. Percent *rho*- or *rho0* colonies was calculated by the formula  $100 \times [1 - (\text{respiratory colonies}/\text{total colonies})]$ . B. Diagram of screen for HS alleles. *Rho*+ cells were treated with 5 $\mu$ g/ml EtBr for 100 minutes to create a mixed mtDNA population, plated to single colonies on YEPD (1% yeast extract, 2% peptone, 2% glucose), mated with lawns of *rho*+ yeast on YEPD, selected for diploids on SD-His-Leu, and plated on YEPD plates with no added adenine. Red colonies on the low adenine YEPD plate are *rho*+ and white colonies are *rho*- or *rho0*. White colonies were taken for further analysis. C. HS candidates tested for mtDNA inheritance bias by quantitative mating assay. HS candidates or a *rho0* control were mated with a *rho*+ tester and selected for diploids colonies which were assessed for *rho*+ mtDNA.

(TIF)

**S2 Fig. PCR detection limits for *Rho*+ loci.** Genomic DNA was isolated from *rho*+ or *HS ORI5-1* parent patches and normalized. *Rho*+ genomic DNA was diluted into *HS ORI5-1* genomic DNA in five-fold serial dilutions. PCRs of using primer sets recognizing mitochondrial loci were performed from the serial dilutions and run on agarose gels containing ethidium bromide. The first lane contains the ladder and the last lane is a no DNA control.

(TIF)

**S3 Fig. *PET127* is the Cause of Suppression by High-Copy Plasmids.** A. Inserts of four plasmids obtained from the high-copy suppressor screen were PCRed using Q5 (New England Biolabs) and Sanger sequenced using the Yep13 backbone primer set. The resulting sequences were identified via NCBI blast [63] and the genomic boundaries of each plasmid insert are as indicated. Parentheses indicate annotated genes contained within the genomic region with 3' or 5' indicating that the genic region was cut off and only the 3' or 5' end of the gene was present. B. The suppressive capability of the high-copy *PET127* plasmid was tested on *HS ORI5* alleles cytoduced into a common recipient strain so as to confirm that the extent of high-copy *PET127* suppression is determined by the HS allele and not by a possible nuclear mutation. C. Typical plates following quantitative inheritance assay. "Total Diploid" images taken 2 days after plating on SD-His-Leu diploid selection medium. "Respiratory" images taken 3 days after replica plating to YEPG. Inset showing colony section growth.

(TIF)

**S4 Fig. Mitochondrial RNA Sequencing Profile of *pet127-ND* Allele Mimics that of *pet127A*.** Mitochondrial gene expression analysis of A. Intragenic mtDNA regions with and

without *COX1* as *COX1* has much higher expression relative to the other mitochondrial genes. B. Non-coding RNA regions: *tRNA* and *ORI*. C. Intergenic mtDNA regions. \* indicates a discovery in both comparisons *WT* to *pet127-ND/pet127Δ* and *WT* to *pet127Δ* via multiple unpaired T-tests with Two-stage step-up (N = 3). “x” indicates discovery in only *WT* to *pet127Δ*. + indicates discovery in only *WT* to *pet127-ND/pet127Δ*. No discoveries were identified in *WT* to *WT/pet127-ND*. Region delineations can be found in [Table 4](#).

(TIF)

**S5 Fig. The *pet127-nd* Suppresses HS Biased Inheritance.** Quantitative mtDNA inheritance assay with high-copy *pet127-nd*. Significance was determined using one-way ANOVA separately on each *HS* and *rho0* cross with means compared to the vector control using Dunnett’s multiple comparison’s test (N = 3). \*\*\*\* indicates adjusted P-value less than 0.0001. All other comparisons were not significantly different.

(TIF)

**S6 Fig. Diagram of tested *PET127* truncation alleles.** Diagram of tested *PET127* truncation constructs in the bacterial expression and binding assay. First row is full length *PET127* with predicted mitochondrial targeting sequence. Second row is with the mitochondrial targeting sequence replaced with 6xHis. All the following rows are truncation alleles to scale. Columns indicate whether the allele was able to express in bacteria or subsequently bind with Rpo41 as in [Fig 4B](#).

(TIF)

**S7 Fig. *PET127* truncation alleles are able to get into the mitochondrion.** Cycling mutant *PET127* and *TOM70-GFP* carrying cells in YEPD were lysed by zymolyase treatment and Dounce homogenization. Mitochondria was enriched by differential centrifugation and 3μg of mitochondria was treated with 50μg/ml proteinase K for 5mins at 37°C. The reaction was stopped by addition of TCA to 12.5%. Samples were immunoblotted as indicated. A low exposure was used for Pet127<sup>1-215</sup>-HA because it was more abundant than Pet127-HA and Pet127<sup>Δ48-215</sup>-HA. Arrows indicate the expected size of Pet127 full length and Pet127<sup>Δ48-215</sup>-HA respectively.

(TIF)

**S8 Fig. *PET127* Overexpression Inhibits *RPO41* Transcription.** A. RT-qPCR of either *COX3*, *COX2* or *ATP9* divided by *ACT1* RNA and normalized by the qPCR of the respective gene divided by *ACT1* DNA. RT-qPCRs were performed on the high-copy *PET127* high-copy *RPO41* combination strains collected at high cell density to increase respiration. The left RT-qPCRs are normalized to the *Vectors* averages. The right column is the same data visualized as a log<sub>2</sub> fold change relative to the *Vectors* control. Significance was determined using one-way ANOVA comparing all values with each other using Tukey’s multiple comparison’s test (N = 2). \*\*\*\* indicates adjusted P-value less than 0.0001, \*\*\* indicates an adjusted P-value less than 0.001, \*\* indicates an adjusted P-value less than 0.01, \* indicates an adjusted P-value less than 0.05. B. qPCR of either *COX3*, *COX2*, or *ATP9* divided by *ACT1* qPCR on DNA isolated from high-copy *PET127* high-copy *RPO41* combination strains. No comparisons were determined as significantly different. Significance was determined using one-way ANOVA comparing all values with each other using Tukey’s multiple comparison’s test (N = 2).

(TIF)

**S9 Fig. *pGal-PET127* Alleles Require Rpo41 Binding Region to Alter Mitochondrial RNA but not *ORI* Transcription.** A. *COX3* RNA RT-qPCR, *COX3* DNA qPCR, or *COX3* RNA RT-qPCR divided by *COX3* DNA qPCR on high-copy *pGal-Pet127* alleles in *rho+* cells normalized

to *ACT1* RNA and/or DNA 0, 3, and 5 hours after addition of galactose. Significance was determined using one-way ANOVA separately for each time point with means compared to either the vector control or the *pGal-mtGFP* control using Dunnett's multiple comparison's test. \*\*\* indicates an adjusted P-value between 0.001 and 0.0001. \* indicates an adjusted P-value between 0.05 and 0.01. All other comparisons were not significantly different. B. Gene expression analysis via RNA sequencing of *PET127* or mitochondrial genic transcripts in cells carrying high-copy *pGal-Pet127* alleles. Values indicate average log<sub>2</sub> fold change between 0 hours and 5 hours after addition of galactose for three independent experiments. C. *ORI* RNA RT-qPCR, *ORI* DNA qPCR, or *ORI* RNA RT-qPCR divided by *ORI* DNA qPCR on high-copy *pGal-Pet127* alleles in *rho+* cells normalized to *ACT1* RNA and/or DNA 0, 3, and 5 hours after addition of galactose. Significance was determined using one-way ANOVA separately for each time point with means compared to either the vector control or the *pGal-mtGFP* control using Dunnett's multiple comparison's test (N = 3). \*\*\*\* indicates an adjusted P-value less than 0.0001. \*\* indicates an adjusted P-value between 0.01 and 0.001. All other comparisons were not significantly different. D. *ORI* RNA RT-qPCR on *HS ORI5-1* and *HS ORI5-2* with *pGal-Pet127* RNA normalized to *ACT1* 0, 3, and 5 hours after addition of galactose. Significance was determined using student's T-test comparing equivalent time points between strains containing either the same *ORI* or *pGal-PET127* allele (N = 2 or 3). \* indicates a P-value between 0.05 and 0.01. All other comparisons were not significant.

(TIF)

**S10 Fig. Pet127 Protein is Less Abundant in Respiratory Conditions and More Abundant in Glucose Medium.** A. Left panel: *PET127-HA V5-RPO41* cells were grown to high cellular density in YEPD medium and samples were collected and immunoblotted for HA, V5 and VDAC. Right panel: A high density culture of *PET127-HA V5-RPO41* cells in YEPD medium was diluted at 0h to  $3.3 \times 10^6$  cells/ml in YEPD medium and samples were collected over time and immunoblotted for HA, V5 and VDAC. B. *PET127-HA V5-RPO41* cells were grown in YEPD medium to mid log, a sample was taken and then the culture was split into YEP medium containing either 2% Glucose, 2% Glycerol, 2% Potassium Acetate, or 2% Ethanol. Samples were taken after 4 hours and samples were stained with Ponceau S and immunoblotted for HA, V5 and VDAC.

(TIF)

**S11 Fig. Synthetic lethality of *rpo41-EI* at 37°C on synthetic dropout medium.** Five-fold serial dilutions of strains containing *RPO41* alleles beginning at  $1.1 \times 10^7$  cells/ml plated on SD-His and incubated at either 30°C, 34°C, or 37°C for 2 days.

(TIF)

## Acknowledgments

We thank Dmitriy Markov for insight about RPO41 allele design, the MIT Biomicro Center and Stuart Levine for the Illumina sequencing experiments and discussions about experimental design of the SMRT and mitochondrial RNA sequencing, Charlie Whittaker and Duanduan Ma of the Barbara K. Ostrom (1978) Bioinformatics and Computing Facility at the Koch Institute in the Swanson Biotechnology Center for sequencing analysis of the SMRT sequencing and RNA sequencing experiments respectively, Maria Zapp and Ellen Kittler of the UMMS Deep Sequencing and Molecular Biology Core Laboratories and the PacBio Core Enterprise for SMRT sequencing, Xiaoxue Zhou for taking the image of [S11 Fig](#), Stephen P. Bell and Matthew Vander Heiden for mentorship and critical reading of the manuscript, and Hilla Weidberg, Xiaoxue Zhou, and John Replogle for critical reading of the manuscript.

## Author Contributions

**Conceptualization:** Daniel Corbi, Angelika Amon.

**Formal analysis:** Daniel Corbi.

**Funding acquisition:** Angelika Amon.

**Investigation:** Daniel Corbi.

**Methodology:** Daniel Corbi.

**Project administration:** Angelika Amon.

**Resources:** Angelika Amon.

**Supervision:** Angelika Amon.

**Writing – original draft:** Daniel Corbi.

**Writing – review & editing:** Daniel Corbi.

## References

1. Veatch JR, McMurray M a, Nelson, Gottschling DE. Mitochondrial dysfunction leads to nuclear genome instability via an iron-sulfur cluster defect. *Cell* [Internet]. 2009 Jun 26 [cited 2014 Aug 7]; 137(7):1247–58. Available from: <http://www.pubmedcentral.nih.gov/articlerender.fcgi?artid=2759275&tool=pmcentrez&rendertype=abstract> <https://doi.org/10.1016/j.cell.2009.04.014> PMID: 19563757
2. Schatz G. Mitochondria: beyond oxidative phosphorylation. *Biochim Biophys Acta*. 1995; 1271:123–6. [https://doi.org/10.1016/0925-4439\(95\)00018-y](https://doi.org/10.1016/0925-4439(95)00018-y) PMID: 7599197
3. Ernster L, Schatz G. Mitochondria: A historical review. *J Cell Biol*. 1981; 91(3 II). <https://doi.org/10.1083/jcb.91.3.227s> PMID: 7033239
4. Chacinska A, Koehler CM, Milenkovic D, Lithgow T, Pfanner N. Importing Mitochondrial Proteins: Machineries and Mechanisms. *Cell*. 2009; 138(4):628–44. <https://doi.org/10.1016/j.cell.2009.08.005> PMID: 19703392
5. Neupert W, Herrmann JM. Translocation of proteins into mitochondria. *Annu Rev Biochem*. 2007; 76:723–49. <https://doi.org/10.1146/annurev.biochem.76.052705.163409> PMID: 17263664
6. Foury F, Roganti T, Lecrenier N, Purnelle B. The complete sequence of the mitochondrial genome of *Saccharomyces cerevisiae*. *FEBS Lett*. 1998; 440(3):325–31. [https://doi.org/10.1016/s0014-5793\(98\)01467-7](https://doi.org/10.1016/s0014-5793(98)01467-7) PMID: 9872396
7. Turk EM, Das V, Seibert RD, Andrulis ED. The Mitochondrial RNA Landscape of *Saccharomyces cerevisiae*. *PLoS One*. 2013; 8(10):1–21. <https://doi.org/10.1371/journal.pone.0078105> PMID: 24143261
8. Conrad MN, Newlon CS. The regulation of mitochondrial DNA levels in *Saccharomyces cerevisiae*. *Curr Genet*. 1982; 6(2):147–52. <https://doi.org/10.1007/BF00435214> PMID: 24186481
9. Maleszka R, Skelly PJ, Clark-Walker GD. Rolling circle replication of DNA in yeast mitochondria. *EMBO J* [Internet]. 1991; 10(12):3923–9. Available from: <http://www.pubmedcentral.nih.gov/articlerender.fcgi?artid=453131&tool=pmcentrez&rendertype=abstract> PMID: 1935911
10. Dujon B. Mitochondrial genetics and function. In: Strathern JN, Jones EW, Broach JR, editors. *The molecular biology of the yeast Saccharomyces: life cycle and inheritance*. Cold Spring Harbor, N.Y.: Cold Spring Harbor Laboratory Press; 1981. p. 505–635.
11. Slonimski PP, Perrodin G, Croft JH. Ethidium bromide induced mutation of yeast mitochondria: Complete transformation of cells into respiratory deficient non-chromosomal “petites.” *Biochem Biophys Res Commun*. 1968; 30(3):232–9. [https://doi.org/10.1016/0006-291x\(68\)90440-3](https://doi.org/10.1016/0006-291x(68)90440-3) PMID: 5647224
12. Slonimski P, Ephrussi B. Action de l'acriflavine sur les levures. V. Le système des cytochromes des mutants ‘petite colonie’ de la levure. *Ann Inst Pasteur (Paris)*. 1949; 77:47–64.
13. Falkenberg M. Mitochondrial DNA replication in mammalian cells: Overview of the pathway. *Essays Biochem*. 2018; 62(3):287–96. <https://doi.org/10.1042/EBC20170100> PMID: 29880722
14. Osman C, Noriega TR, Okreglak V, Fung JC, Walter P. Integrity of the yeast mitochondrial genome, but not its distribution and inheritance, relies on mitochondrial fission and fusion. *Proc Natl Acad Sci [Internet]*. 2015;201501737. Available from: <http://www.pnas.org/lookup/doi/10.1073/pnas.1501737112>

15. Nunnari J, Marshall W, Straight A, Murray A, Sedat J, Walter P. Mitochondrial transmission during mating in *S. cerevisiae* is determined by mitochondrial fusion and fission and the intramitochondrial segregation of mtDNA. *Mol Biol Cell*. 1997; 8(7):1233–42. <https://doi.org/10.1091/mbc.8.7.1233> PMID: 9243504
16. Murley A, Lackner LL, Osman C, West M, Voeltz GK, Walter P, et al. ER-associated mitochondrial division links the distribution of mitochondria and mitochondrial DNA in yeast. *Elife* [Internet]. 2013 Jan [cited 2014 Sep 15]; 2:e00422. Available from: <http://www.pubmedcentral.nih.gov/articlerender.fcgi?artid=3654481&tool=pmcentrez&rendertype=abstract> <https://doi.org/10.7554/eLife.00422> PMID: 23682313
17. Labbé K, Murley A, Nunnari J. Determinants and Functions of Mitochondrial Behavior. *Annu Rev Cell Dev Biol* [Internet]. 2014; 30:357–91. Available from: <http://www.annualreviews.org/doi/abs/10.1146/annurev-cellbio-101011-155756> PMID: 25288115
18. Ephrussi B, de Margerie-Hottinguer H, Roman H. Suppressiveness: a New Factor in the Genetic Determinism of the Synthesis of Respiratory Enzymes in Yeast. *Proc Natl Acad Sci U S A*. 1955; 41(12):1065–71. <https://doi.org/10.1073/pnas.41.12.1065> PMID: 16589797
19. Goursot R, de Zamaroczy M, Baldacci G, Bernardi G. Supersuppressive “petite” mutants of yeast. *Curr Genet*. 1980; 1(2):173–6. <https://doi.org/10.1007/BF00446963> PMID: 24190841
20. Ephrussi B, Grandchamp S. ETUDES SUR LA SUPPRESSIVITE DES MUTANTS A DEFICIENCE RESPIRATOIRE DE LA LEVURE. *Heredity (Edinb)*. 1965; 20(February):1–7. <https://doi.org/10.1038/hdy.1965.1> PMID: 14302072
21. Mikklos De Zamaroczy Giuseppe Baldacci and GB. Putative Origins of Replication in the Mitochondrial Genome of Yeast. *FEBS Lett*. 1979; 102(2):429–32.
22. Blanc H, Dujon B. Replicator regions of the yeast mitochondrial DNA responsible for suppressiveness. *Proc Natl Acad Sci U S A*. 1980; 77(July 1980):3942–6. <https://doi.org/10.1073/pnas.77.7.3942> PMID: 7001449
23. Blanc H, Dujon B. Replicator regions of the yeast mitochondrial DNA active in vivo and in yeast transformants. In: Slonimski P, Borst P, Attardi G, editors. *Mitochondrial genes*. Cold Spring Harbor, NY: Cold Spring Harbor Laboratory Press; 1982. p. 279–94.
24. Gingold EB. Genetic analysis of the products of a cross involving a suppressive “petite” mutant of *S. cerevisiae*. *Curr Genet*. 1981; 3(3):213–20. <https://doi.org/10.1007/BF00429823> PMID: 24190133
25. Schmitt ME, Clayton DA. Conserved features of yeast and mammalian mitochondrial DNA replication. *Curr Opin Genet Dev*. 1993; 3(5):769–74. [https://doi.org/10.1016/s0959-437x\(05\)80097-8](https://doi.org/10.1016/s0959-437x(05)80097-8) PMID: 8274861
26. Shadel GS, Clayton DA. Mitochondrial DNA Maintenance in Vertebrates. *Annu Rev Biochem*. 1997; 66:409–35. <https://doi.org/10.1146/annurev.biochem.66.1.409> PMID: 9242913
27. Baldacci G, Bernardi G. Replication origins are associated with transcription initiation sequences in the mitochondrial genome of yeast. *EMBO J*. 1982; 1(8):987–94. PMID: 6329719
28. Dyck E Van Clayton DA. Transcription-Dependent DNA Transactions in the Mitochondrial Genome of a Yeast Hypersuppressive Petite Mutant. *Mol Cell Biol*. 1998; 18(5):2976–85. <https://doi.org/10.1128/MCB.18.5.2976> PMID: 9566917
29. Stohl LL, Clayton D a. *Saccharomyces cerevisiae* contains an RNase MRP that cleaves at a conserved mitochondrial RNA sequence implicated in replication priming. *Mol Cell Biol*. 1992; 12(6):2561–9. <https://doi.org/10.1128/mcb.12.6.2561-2569.1992> PMID: 1588958
30. Sanchez-Sandoval E, Diaz-Quezada C, Velazquez G, Arroyo-Navarro LF, Almanza-Martinez N, Traviña-Arenas CH, et al. Yeast mitochondrial RNA polymerase primes mitochondrial DNA polymerase at origins of replication and promoter sequences. *Mitochondrion* [Internet]. 2015; 24:22–31. Available from: <http://www.sciencedirect.com/science/article/pii/S1567724915300052> <https://doi.org/10.1016/j.mito.2015.06.004> PMID: 26184436
31. Fangman WL, Henly JW, Churchill G, Brewer BJ. Stable maintenance of a 35-base-pair yeast mitochondrial genome. *Mol Cell Biol*. 1989; 9(5):1917–21. <https://doi.org/10.1128/mcb.9.5.1917-1921.1989> PMID: 2664462
32. Chou JY, Leu JY. The Red Queen in mitochondria: Cyto-nuclear co-evolution, hybrid breakdown and human disease. *Front Genet*. 2015; 6(MAY):1–8. <https://doi.org/10.3389/fgene.2015.00001> PMID: 25674101
33. Wallace DC, Chalkia D. Mitochondrial DNA genetics and the heteroplasmy conundrum in evolution and disease. *Cold Spring Harb Perspect Med*. 2013; 3(10):1–48.
34. Godeleine Faugeron-Fonty, Caroline Le, Van Kim, et al. A comparative study of the ori sequences from the mitochondrial genomes of twenty wild-type yeast strains. *Gene*. 1984; 32:459–73. [https://doi.org/10.1016/0378-1119\(84\)90020-9](https://doi.org/10.1016/0378-1119(84)90020-9) PMID: 6397407

35. de Zamaroczy M, Faugeron-Fonty G, Baldacci G, Goursot R, Bernardi G. The ori sequences of the mitochondrial genome of a wild-type yeast strain: number, location, orientation and structure. *Gene*. 1984; 32(3):439–57. [https://doi.org/10.1016/0378-1119\(84\)90019-2](https://doi.org/10.1016/0378-1119(84)90019-2) PMID: 6397406
36. Fangman WL, Henly JW, Brewer BJ. RPO41-independent maintenance of [rho-] mitochondrial DNA in *Saccharomyces cerevisiae*. *Mol Cell Biol*. 1990; 10(1):10–5. <https://doi.org/10.1128/mcb.10.1.10-15.1990> PMID: 2152961
37. Fangman WL, Dujon B. Yeast mitochondrial genomes consisting of only A.T base pairs replicate and exhibit suppressiveness. *Proc Natl Acad Sci U S A* [Internet]. 1984; 81(22):7156–60. Available from: <http://www.pubmedcentral.nih.gov/articlerender.fcgi?artid=392096&tool=pmcentrez&rendertype=abstract> <https://doi.org/10.1073/pnas.81.22.7156> PMID: 6390432
38. Lorimer HE, Brewer BJ, Fangman WL. A test of the transcription model for biased inheritance of yeast mitochondrial DNA. *Mol Cell Biol*. 1995; 15(9):4803–9. <https://doi.org/10.1128/MCB.15.9.4803> PMID: 7651397
39. Ling F, Hori A, Shibata T. DNA recombination-initiation plays a role in the extremely biased inheritance of yeast [rho-] mitochondrial DNA that contains the replication origin ori5. *Mol Cell Biol*. 2007; 27(November):1133–45. <https://doi.org/10.1128/MCB.00770-06> PMID: 17116696
40. Ling F, Hori A, Yoshitani A, Niu R, Yoshida M, Shibata T. Din7 and Mhr1 expression levels regulate double-strand-break-induced replication and recombination of mtDNA at ori5 in yeast. *Nucleic Acids Res*. 2013; 41(April):5799–816. <https://doi.org/10.1093/nar/gkt273> PMID: 23598996
41. Chambers P, Gingold E. A direct study of the relative synthesis of petite and grande petite mutants of *Saccharomyces cerevisiae*. *Curr Genet*. 1986; 10:565–71. <https://doi.org/10.1007/BF00418122> PMID: 3327610
42. Bradshaw E, Yoshida M, Ling F. Regulation of Small Mitochondrial DNA Replicative Advantage by Ribonucleotide Reductase in *Saccharomyces cerevisiae*. *Genes[Genomes]Genetics* [Internet]. 2017; 7(September 2017):3083–90. Available from: <http://g3journal.org/lookup/doi/10.1534/g3.117.043851> PMID: 28717049
43. Lai-Zhang J, Xiao Y, Mueller DM. Epistatic interactions of deletion mutants in the genes encoding the F1-ATPase in yeast *Saccharomyces cerevisiae*. *EMBO J*. 1999; 18(1):58–64. <https://doi.org/10.1093/emboj/18.1.58> PMID: 9878050
44. MacAlpine DM, Kolesar J, Okamoto K, Butow R a, Perlman PS. Replication and preferential inheritance of hypersuppressive petite mitochondrial DNA. *EMBO J* [Internet]. 2001 Apr 2; 20(7):1807–17. Available from: <http://www.pubmedcentral.nih.gov/articlerender.fcgi?artid=145480&tool=pmcentrez&rendertype=abstract> <https://doi.org/10.1093/emboj/20.7.1807> PMID: 11285243
45. DeMarini DJ, Adams AEM, Fares H, De Virgilio C, Valle G, Chuang JS, et al. A Septin-based Hierarchy of Proteins Required for Localized Deposition of Chitin in the *Saccharomyces cerevisiae* Cell Wall. *J Cell Biol*. 1997; 139(1):75–93. <https://doi.org/10.1083/jcb.139.1.75> PMID: 9314530
46. Wiesenberger G, Fox TD. Pet127p, a membrane-associated protein involved in stability and processing of *Saccharomyces cerevisiae* mitochondrial RNAs. *Mol Cell Biol*. 1997; 17(5):2816–24. <https://doi.org/10.1128/MCB.17.5.2816> PMID: 9111353
47. Karavaeva IE, Golyshev SA, Smirnova EA, Sokolov SS, Severin FF, Knorre DA. Mitochondrial depolarization in yeast zygotes inhibits clonal expansion of selfish mtDNA. *J Cell Sci*. 2017; 130(7):1274–84. <https://doi.org/10.1242/jcs.197269> PMID: 28193734
48. Lancashire WE, Mattoon JR. Cytoduction : A Tool for Mitochondrial Genetic Studies in Yeast. 1979; 344:333–44. <https://doi.org/10.1007/BF00267067> PMID: 379549
49. Haffter P, Fox TD. Suppression of carboxy-terminal truncations of the yeast mitochondrial mRNA-specific translational activator PET122 by mutations in two new genes, MRP17 and PET127. *MGG Mol Gen Genet*. 1992; 235(1):64–73. <https://doi.org/10.1007/BF00286182> PMID: 1279374
50. Margelevičius M, Laganeckas M, Venclovas Č. COMA server for protein distant homology search. *Bioinformatics*. 2010; 26(15):1905–6. <https://doi.org/10.1093/bioinformatics/btq306> PMID: 20529888
51. Fekete Z, Ellis TP, Schonauer MS, Dieckmann CL. Pet127 governs a 5'→3'-exonuclease important in maturation of apocytochrome b mRNA in *Saccharomyces cerevisiae*. *J Biol Chem*. 2008; 283(7):3767–72. <https://doi.org/10.1074/jbc.M709617200> PMID: 18086665
52. Islas-Osuna M a., Ellis TP, Marnell LL, Mittelmeier TM, Dieckmann CL. Cbp1 is required for translation of the mitochondrial cytochrome b mRNA of *Saccharomyces cerevisiae*. *J Biol Chem*. 2002; 277(41):37987–90. <https://doi.org/10.1074/jbc.M206132200> PMID: 12149267
53. Markov DA, Savkina M, Anikin M, Del Campo M, Ecker K, Lambowitz AM, et al. Identification of proteins associated with the yeast mitochondrial RNA polymerase by tandem affinity purification. *Yeast*. 2009; 26(10):423–40. <https://doi.org/10.1002/yea.1672> PMID: 19536766

54. Claros MG, Vincens P. Computational method to predict mitochondrially imported proteins and their targeting sequences. *Eur J Biochem*. 1996; 241(3):779–86. <https://doi.org/10.1111/j.1432-1033.1996.00779.x> PMID: 8944766
55. Mohd Azhar SH, Abdulla R, Jambo SA, Marbawi H, Gansau JA, Mohd Faik AA, et al. Yeasts in sustainable bioethanol production: A review. *Biochem Biophys Reports*. 2017; 10(February):52–61. <https://doi.org/10.1016/j.bbrep.2017.03.003> PMID: 29114570
56. Dombek KM, Ingram LO. Ethanol production during batch fermentation with *Saccharomyces cerevisiae*: Changes in glycolytic enzymes and internal pH. *Appl Environ Microbiol*. 1987; 53(6):1286–91. <https://doi.org/10.1128/aem.53.6.1286-1291.1987> PMID: 3300550
57. Galdieri L, Mehrotra S, Yu S, Vancura A. Transcriptional regulation in yeast during diauxic shift and stationary phase. *Omi A J Integr Biol*. 2010; 14(6):629–38. <https://doi.org/10.1089/omi.2010.0069> PMID: 20863251
58. Greenleaf AL, Kelly JL, Lehman IR. Yeast RPO41 gene product is required for transcription and maintenance of the mitochondrial genome. *Proc Natl Acad Sci U S A* [Internet]. 1986; 83(10):3391–4. Available from: <http://www.ncbi.nlm.nih.gov/pubmed/3517858> <http://www.ncbi.nlm.nih.gov/pmc/articles/PMC323519/pdf/pnas00314-0350.pdf> <https://doi.org/10.1073/pnas.83.10.3391> PMID: 3517858
59. Dujon B, Slonimski PP, Weill L. Mitochondrial genetics. IX. A model for recombination and segregation of mitochondrial genomes in *Saccharomyces cerevisiae*. *Genetics*. 1974; 78(1):415–37. <https://doi.org/10.1093/genetics/78.1.415> PMID: 4613610
60. Blitzblau HG, Chan CS, Hochwagen A, Bell SP. Separation of DNA replication from the assembly of break-competent meiotic chromosomes. *PLoS Genet*. 2012;8(5). <https://doi.org/10.1371/journal.pgen.1002643> PMID: 22615576
61. Hamperl S, Bocek MJ, Saldivar JC, Swigut T, Cimprich KA. Transcription-Replication Conflict Orientation Modulates R-Loop Levels and Activates Distinct DNA Damage Responses. *Cell* [Internet]. 2017; 170(4):774–786.e19. Available from: <http://dx.doi.org/10.1016/j.cell.2017.07.043> PMID: 28802045
62. Wanrooij PH, Engqvist MKM, Forslund JME, Navarrete C, Nilsson AK, Sedman J, et al. Ribonucleotides incorporated by the yeast mitochondrial DNA polymerase are not repaired. *Proc Natl Acad Sci U S A*. 2017; 114(47):12466–71. <https://doi.org/10.1073/pnas.1713085114> PMID: 29109257
63. Zhang Z, Schwartz S, Wagner L, Miller W. A greedy algorithm for aligning DNA sequences. *J Comput Biol*. 2000; 7(1–2):203–14. <https://doi.org/10.1089/10665270050081478> PMID: 10890397
64. Longtine MS, McKenzie a, Demarini DJ, Shah NG, Wach a, Brachat a, et al. Additional modules for versatile and economical PCR-based gene deletion and modification in *Saccharomyces cerevisiae*. *Yeast* [Internet]. 1998 Jul; 14(10):953–61. Available from: <http://www.ncbi.nlm.nih.gov/pubmed/9717241> [https://doi.org/10.1002/\(SICI\)1097-0061\(199807\)14:10<953::AID-YEA293>3.0.CO;2-U](https://doi.org/10.1002/(SICI)1097-0061(199807)14:10<953::AID-YEA293>3.0.CO;2-U) PMID: 9717241
65. Gibson DG. Enzymatic assembly of overlapping DNA fragments. *Methods Enzymol*. 2011; 498:349–61. <https://doi.org/10.1016/B978-0-12-385120-8.00015-2> PMID: 21601685
66. Rose MD, Winston F, Hieter P. *Methods in Yeast Genetics: A Laboratory Course Manual*. Schweitzer B, Philippsen P, editors. Cold Spring Harbor, New York: Cold Spring Harbor Laboratory Press; 1990.
67. Corbi D, Amon A. SMRT sequencing data on four hypersuppressive *Saccharomyces cerevisiae* mitochondrial DNAs. [Internet]. Dryad Digital Repository. Durham (NC): Dryad; 2021 [cited 2021 Oct 11]. Available from: <https://datadryad.org/stash/>
68. Robinson JT, Thorvaldsdóttir H, Winckler W, Guttman M, Lander ES, Getz G, et al. Integrative genomics viewer. *Nat Biotechnol*. 2011; 29(1):24–6. <https://doi.org/10.1038/nbt.1754> PMID: 21221095
69. Corbi D, Amon A. RNA sequencing of nuclease dead PET127 conditions [Internet]. Dryad Digital Repository. Durham (NC): Dryad; 2021 [cited 2021 Oct 11]. Available from: <https://datadryad.org/stash/>
70. Corbi D, Amon A. RNA sequencing of PET127 mutants overexpressed using the galactose inducible promoter [Internet]. Dryad Digital Repository. Durham (NC): Dryad; 2021 [cited 2021 Oct 11]. Available from: <https://datadryad.org/stash/>
71. Pfanner N., Meisinger C., Turcotte B., in *Yeast Protocols*, Xiao W., Ed. (Springer, 2006), vol. 313 pp. 33–39. *Yeast Protocols 2nd Ed. Vol. 1, Methods in molecular Biology*. 2006. 408 p.